

ARTICLE TYPE

Guided structure learning of DAGs for count data

Thi Kim Hue NGUYEN*¹ | Monica Chiogna² | Davide Risso¹ | Erika Banzato¹¹Department of Statistical Sciences,
University of Padova, Padova, Italy²Department of Statistical Sciences
“Paolo Fortunati”, University of
Bologna, Bologna, Italy

Correspondence

*Thi Kim Hue NGUYEN Email:
nguyen@stat.unipd.it

Summary

In this paper, we tackle structure learning of Directed Acyclic Graphs (DAGs), with the idea of exploiting available prior knowledge of the domain at hand to guide the search of the best structure. In particular, we assume to know the topological ordering of variables in addition to the given data. We study a new algorithm for learning the structure of DAGs, proving its theoretical consistence in the limit of infinite observations. Furthermore, we experimentally compare the proposed algorithm to a number of popular competitors, in order to study its behavior in finite samples.

KEYWORDS:

Consistency, Directed acyclic graphs, Graphical models, Guided structure learning, Topological ordering

1 | INTRODUCTION

Current demand for modelling complex interactions between variables, combined with the greater availability of high-dimensional discrete data, possibly showing a large number of zeros and measured on a small number of units, has led to an increased focus on structure learning for discrete data in high dimensional settings. In some applications, directed graphs are preferable, as they translate naturally into domain-specific concepts. For instance, when modeling interactions among genes, an arrow between two nodes describes a hierarchical interaction between the corresponding two genes. Hence, the problem often specializes in structure learning of Directed Acyclic Graphs (DAGs).

Some solutions are nowadays available in the literature for learning (sparse) DAGs for discrete data. Hadiji, Molina, Natarajan, and Kersting (2015) introduce a novel family of non-parametric Poisson graphical models, called Poisson Dependency Networks (PDN), trained using functional gradient ascent; Park and Raskutti (2015) define general Poisson DAG models which are identifiable from observational data, and present a polynomial-time algorithm that learns the Poisson DAG model under suitable regularity conditions.

The previously cited approaches, and, more broadly, typical approaches to structure learning of DAGs, usually assume no knowledge of the graph structure to be learned other than sparseness. However, in the context of learning gene networks, a wealth of information is actually available, usually stored in repositories such as KEGG (Kanehisa & Goto 2000), about a myriad of interactions, reactions, and regulations. Such information is often identified piecemeal over extended periods and by a variety of researchers, and can therefore be not fully precise. Nevertheless, it allows to order variables following directional relationships.

When the ordering of variables is known, then the strategy of neighborhood recovery turns the problem of learning the structure of a DAG into a straightforward task. The graph selection problem is split into a sequence of feature selection problems by assuming that the conditional distribution of each variable given its precedents in the topological ordering follows the chosen distribution. To learn the structure of a DAG, it is sufficient to perform a (sparse) regression for each variable, treating all preceding variables as covariates. It is known that simply performing lasso-type ℓ_1 -penalized regressions yields consistency for both the coefficients and the sparsity pattern (the set of nonzero coefficients) in regression (Li, Scarlett, Ravikumar, & Cevher 2015), and thus, yields consistency for the DAG structure.

The idea of assuming a known ordering of the variables is not novel and several authors have considered decoupling the search over orderings from the graph estimation given the ordering. However, coming up with a good ordering of variables usually requires a significant

amount of domain knowledge, which is not commonly available in many practical applications. As a consequence, various approaches exploiting the topological ordering of the variables implement, in different ways, a search over the space of topological orderings. In the Gaussian setting, Bühlmann, Peters, and Ernest (2014) estimate a superset of the skeleton of the underlying DAG, then search a topological ordering using (restricted) maximum likelihood estimation based on an additive structural equation model with Gaussian errors, and finally, exploiting the estimated order of the variables, use sparse additive regression to estimate the functions in an additive structural equation model. Teyssier and Koller (2005) propose to learn a DAG by a search not over the space of structures, but over the space of orderings, selecting for each ordering the most consistent network (OS algorithm); Schmidt, Niculescu-Mizil, and Murphy (2007) couple the OS algorithm with a sparsity-promoting ℓ_1 -regularization.

In this work, we propose one algorithm for structure learning of DAGs for count data which is not affected by non uniqueness of the topological ordering and overcomes some of the shortcomings induced by the use of penalized procedures. It is the case, in fact, that penalization is scale-variant, a condition that often interferes with some of the filtering steps that are commonly performed in the analysis of complex datasets, such as those arising in genomics. Moreover, it could suffer from over-shrinking of small but significant covariate effects. Our proposal, named Or-PPGM (PC-based learning of Oriented Poisson Graphical Models), is based on a modification of the PC algorithm (Kalisch & Bühlmann 2007). In Or-PPGM, we assume to know whether a variable, *i* say, comes before or after *j* ($i \neq j$) in an ordering of the available variables that describes the fundamental mechanisms operative in the physical situation. Furthermore, we substitute penalized estimation of the local regressions with a testing procedure on the regression parameters, following the lines of the PC algorithm. Provided that the assumed topological ordering belongs to the space of true topological orderings, we give a theoretical proof of convergence of Or-PPGM that shows that the proposed algorithm consistently estimates the edges of the underlying DAG, as the sample size $n \rightarrow \infty$, irrespective of the choice of the topological ordering. The iterative testing procedure performed within the PC algorithm allows to guarantee scale-invariance of the procedure and avoids over-shrinking of small effects.

The paper is organized as follows. Some essential concepts on DAG models and Poisson DAG models are given in Section 2. Section 3 is devoted to the illustration of the proposed algorithm. We then provide statistical guarantees in Section 4, and, in Section 5, experimental results that illustrate the performance of our methods in finite samples. Section 6 provides an application to gene expression data. Some conclusions and remarks are provided in Section 7. Results needed to prove the two main theorems in the paper, two other structure learning algorithms and additional simulation results can be found in Supplementary Material.

2 | BACKGROUND ON POISSON DAG MODELS

In this section, we review, setting up the required notation, some essential concepts on DAG models and present Poisson DAG models according to the model specification introduced by Park and Raskutti (2015).

Consider a p -dimensional random vector $\mathbf{X} = (X_1, \dots, X_p)$ such that each random variable X_s corresponds to a node of a directed graph $G = (V, E)$ with index set $V = \{1, 2, \dots, p\}$. A directed edge from node k to node j is denoted by $k \rightarrow j$, k is called a parent of node j , and j is a child of k . The set of parents of a vertex j , denoted $\text{pa}(j)$, consists of all parents of node j ; its descendants, i.e., nodes that can be reached from j by repeatedly moving from parent to child, are denoted $\text{de}(j)$. Non-descendants of j are $\text{nd}(j) = V \setminus (\{j\} \cup \text{de}(j))$.

A DAG is a directed graph that does not have any directed cycles. In other words, there is no pair (j, k) such that there are directed paths from j to k and from k to j . A topological ordering j_1, \dots, j_p is an order of p nodes such that there are no directed paths from j_k to j_t if $k > t$.

In a DAG, independence is encoded by the relation of *d*-separation, defined as in Lauritzen (1996). A random vector \mathbf{X} satisfies the local Markov property with respect to (w.r.t.) a DAG G if $X_v \perp\!\!\!\perp \mathbf{X}_{\text{nd}(v) \setminus \text{pa}(v)} | \mathbf{X}_{\text{pa}(v)}$ for every $v \in V$. Similarly, \mathbf{X} satisfies the global Markov property w.r.t. G if $\mathbf{X}_A \perp\!\!\!\perp \mathbf{X}_B | \mathbf{X}_C$ for all triples of pairwise disjoint subsets $A, B, C \subset V$ such that C *d*-separates A and B in G , which we denote by $A \perp\!\!\!\perp_G B | C$. In this work, we take the assumption that the DAG G is a perfect map, that is, it satisfies the global Markov property and its reverse implication, known as faithfulness. A distribution $P_{\mathbf{X}}$ is said to be faithful to graph G if $\mathbf{X}_A \perp\!\!\!\perp \mathbf{X}_B | \mathbf{X}_C \Rightarrow A \perp\!\!\!\perp_G B | C$, for all disjoint vertex sets A, B, C .

In the Poisson case, the distribution of \mathbf{X} has the form

$$\begin{aligned} \mathbb{P}_{\boldsymbol{\theta}}(\mathbf{x}) &= \prod_{s=1}^p \mathbb{P}_{\theta_s}(x_s | \mathbf{x}_{\text{pa}(s)}) \\ &= \exp \left\{ \sum_{s=1}^p \sum_{t \in \text{pa}(s)} \theta_{st} x_s x_t - \sum_{s=1}^p \log(x_s!) - \sum_{s=1}^p e^{\sum_{t \in \text{pa}(s)} \theta_{st} x_t} \right\}. \end{aligned} \tag{1}$$

where $\theta_s = \{\theta_{st}, s, t \in V, t \neq s\}$ and $\theta = \{\theta_s, s \in V\}$ denotes the set of conditional dependence parameters of the local Poisson regression models characterizing the conditional densities $\mathbb{P}_{\theta_s}(X_s | \mathbf{x}_{\text{pa}(s)})$,

$$\begin{aligned} \mathbb{P}_{\theta_s}(X_s | \mathbf{x}_{\text{pa}(s)}) &= \exp \left\{ \sum_{t \in \text{pa}(s)} \theta_{st} X_s X_t - \log(x_s!) - e^{\sum_{t \in \text{pa}(s)} \theta_{st} X_t} \right\} \\ &= \exp \left\{ \mathbf{x}_s \langle \theta_s, \mathbf{x}_{V \setminus \{s\}} \rangle - \log(x_s!) - D(\langle \theta_s, \mathbf{x}_{V \setminus \{s\}} \rangle) \right\}, \end{aligned} \quad (2)$$

where $\langle \cdot, \cdot \rangle$ denotes the inner product, and $D(\langle \theta_s, \mathbf{x}_{V \setminus \{s\}} \rangle) = e^{\sum_{t \in V \setminus \{s\}} \theta_{st} X_t}$. This specification puts an edge from node t to node s if $\theta_{st} \neq 0$. A missing edge $t \rightarrow s$ corresponds to the condition $\theta_{st} = 0$, implying conditional independence of X_s and X_t given the parents of s , that is, $X_s \perp\!\!\!\perp X_t | \mathbf{x}_{\text{pa}(s)}$. As we are only interested in the structure of graph G , without loss of generality we have assumed that the local Poisson regression models characterizing the conditional densities $\mathbb{P}_{\theta_s}(X_s | \mathbf{x}_{\text{pa}(s)})$ have zero intercept. Specification (2) is similar to that used in Allen and Liu (2013) for the undirected version of Poisson graphical models. The only difference lies in the identification of the parameter space for θ that guarantees existence of the joint distribution. While the distribution represented in (1) is always a valid distribution, in the undirected case a joint distribution compatible with the local specifications exists only if all parameters assume non-positive values.

It is worth noting that, to have a perfect map, it is enough to assume faithfulness of the Poisson node conditional distributions to the graph G , as this guarantees faithfulness of the joint distributions thanks to the equivalence between local and global Markov property.

When the conditional models do not share common parameters, the expression of the joint distribution in (1) suggests that the structure of the network might be recovered from observed data by disjointly maximizing the single factors in the log-likelihood $\ell(\theta, \mathbb{X})$, since the log-likelihood is decomposable as the sum of partial log-likelihoods over all nodes. Therefore, structure learning is based on solving local convex optimization problems. Each local estimated conditional dependence parameter $\hat{\theta}_s$ is then combined to form the global estimate.

3 | THE OR-PPGM ALGORITHM

In this section, we tackle structure learning of DAGs, with the idea of exploiting available prior knowledge of the domain at hand to guide the search for the best structure. In particular, we will assume to know the topological ordering of variables. In what follows, we adopt the convention of using superscripts, e.g., $\mathbf{X}^{(1)}, \dots, \mathbf{X}^{(n)}$, to denote independent copies of the \mathbf{p} -random vector \mathbf{X} , where $\mathbf{X}^{(i)} = (X_{i1}, \dots, X_{ip})$. We denote with $\mathbb{X} = \{\mathbf{x}^{(1)}, \dots, \mathbf{x}^{(n)}\}$ the collection of n observed samples drawn from the random vectors $\mathbf{X}^{(1)}, \dots, \mathbf{X}^{(n)}$, with $\mathbf{x}^{(i)} = (x_{i1}, \dots, x_{ip})$, $i = 1, \dots, n$.

Let i_1, i_2, \dots, i_p indicate one of the possible topological orderings of the variables. The conditional distribution of each variable X_{i_s} given its precedents, denoted $\text{pre}(i_s)$, in the topological ordering i_1, i_2, \dots, i_p can be written as

$$\mathbb{P}_{\theta_{i_s | \text{pre}(i_s) \cup \{i_s\}}}(X_{i_s} | \mathbf{x}_{\text{pre}(i_s)}) = \exp \left\{ \mathbf{x}_{i_s} \langle \theta_{i_s | \text{pre}(i_s) \cup \{i_s\}}, \mathbf{x}_{\text{pre}(i_s)} \rangle - \log(x_{i_s}!) - D(\langle \theta_{i_s | \text{pre}(i_s) \cup \{i_s\}}, \mathbf{x}_{\text{pre}(i_s)} \rangle) \right\}, \quad (3)$$

where $\theta_{s|K} = \{\theta_{st|K} : t \in K, t \neq s\}$, and $\theta_K = \{\theta_{s|K} : s \in K\}$, denote the set of conditional parameters on conditional set K . Then, a rescaled negative node conditional log-likelihood formed by products of all the conditional distributions is as follows

$$\begin{aligned} \ell(\theta_{i_s | \text{pre}(i_s) \cup \{i_s\}}, \mathbb{X}_{i_s}; \mathbb{X}_{\text{pre}(i_s)}) &= -\frac{1}{n} \log \prod_{t=1}^n \mathbb{P}_{\theta_{i_s | \text{pre}(i_s) \cup \{i_s\}}}(X_{i_s}^{(t)} | \mathbf{x}_{\text{pre}(i_s)}^{(t)}) \\ &= \frac{1}{n} \sum_{t=1}^n \left[-X_{i_s}^{(t)} \langle \theta_{i_s | (\text{pre}(i_s) \cup i_s)}, \mathbf{x}_{\text{pre}(i_s)}^{(t)} \rangle - \log(x_{i_s}^{(t)}) - D(\langle \theta_{i_s | \text{pre}(i_s) \cup \{i_s\}}, \mathbf{x}_{\text{pre}(i_s)}^{(t)} \rangle) \right]. \end{aligned} \quad (4)$$

The absence of an edge $t \rightarrow i_s$ implies $\theta_{i_s t | \text{pre}(i_s) \cup \{i_s\}}$ to be equal to zero.

The algorithm Or-PPGM is based on a modification of the well known PC algorithm (Kalisch & Bühlmann 2007). Here, we exploit the idea that consistency of the PC algorithm ultimately depends upon the consistency of the tests of conditional independence employed in the learning process. In our case, consistent tests can be constructed from Wald type tests on the parameters $\theta_{st|K}$ (see also Nguyen and Chiogna (2021)). We combine this idea with that of making use of the topological ordering to determine the sequence of tests to be performed. Assuming that the order of variables is specified beforehand considerably reduces the number of conditional independence tests to be performed. For example, for each $s \in V$, it is sufficient to test if data support existence of the conditional independence relation $X_s \perp\!\!\!\perp X_t | \mathbf{X}_S$ only for $t \in \text{pre}(s)$ and for any $S \subset \{V \cap \text{pre}(s)\} \setminus \{s, t\}$.

The algorithm starts from the complete DAG obtained by directing all edges of a complete undirected graph as suggested by the topological ordering. At each level of the cardinality of the conditioning variable set $\mathbf{K} \setminus \{s\}$, we test, at some pre-specified significance level, the null hypothesis $H_0 : \theta_{st|K} = 0$. If the null hypothesis is not rejected, the edge $t \rightarrow s$ is considered to be absent from the graph. We note that the cardinality of the set $\mathbf{K} \setminus \{s\}$ increases from 0 to $\min\{\text{ord}(s) - 1, m\}$, where $\text{ord}(s)$ is the position of node s in the topological ordering and m an upper bound on the cardinality of conditional sets. For a description of the conditional independence test, as well as the

definition of an appropriate test statistic, we refer readers to Nguyen and Chiogna (2021). The pseudo-code of the Or-PPGM algorithm is given in Algorithm 1.

Algorithm 1 The Or-PPGM algorithm.

```

1: Input:  $n$  independent realizations of the  $\mathbf{p}$ -random vector  $\mathbf{X}$ ,  $\mathbf{x}^{(1)}, \mathbf{x}^{(2)}, \dots, \mathbf{x}^{(n)}$ ; a topological ordering  $\text{Ord}$ , (and a stopping level  $m$ ).
2: Output: An estimated DAG  $\hat{\mathbf{G}}$ .
3: Form the complete undirected graph  $\tilde{\mathbf{G}}$  on the vertex set  $\mathbf{V}$ .
4: Orient edges on  $\tilde{\mathbf{G}}$  to form DAG  $\mathbf{G}'$ .
5:  $l = -1$ ;  $\hat{\mathbf{G}} = \mathbf{G}'$ 
6: repeat
7:    $l = l + 1$ 
8:   for all vertices  $s \in \mathbf{V}$ , do
9:     let  $\mathbf{K}_s = \text{pa}(s)$ 
10:  end for
11:  repeat
12:    Select a (new) edge  $t \rightarrow s$  in  $\hat{\mathbf{G}}$  such that
13:     $|\mathbf{K}_s \setminus \{t\}| \geq l$ .
14:    repeat
15:      choose a (new) set  $\mathbf{S} \subset \mathbf{K}_s \setminus \{t\}$  with  $|\mathbf{S}| = l$ .
16:      if  $\mathbf{H}_0 : \theta_{st|\mathbf{S} \cup \{s\}} = 0$  not rejected
17:        delete edge  $t \rightarrow s$  from  $\hat{\mathbf{G}}$ 
18:      end if
19:    until edge  $t \rightarrow s$  is deleted or all  $\mathbf{S} \subset \mathbf{K}_s \setminus \{t\}$  with  $|\mathbf{S}| = l$  have been considered.
20:  until all edge  $t \rightarrow s$  in  $\hat{\mathbf{G}}$  such that  $|\mathbf{K}_s \setminus \{t\}| \geq l$  and  $\mathbf{S} \subset \mathbf{K}_s \setminus \{t\}$  with  $|\mathbf{S}| = l$  have been tested for conditional independence.
21: until  $l = m$  or for each edge  $t \rightarrow s$  in  $\hat{\mathbf{G}}$ :  $|\mathbf{K}_s \setminus \{t\}| < l$ .

```

Remark 1. As a special case, we consider a variant of Or-PPGM algorithm, called Or-LPGM (Oriented-Local Poisson Graphical Models). In detail, for each $i_s \in \mathbf{V}$, let $\mathbf{S} = \text{pre}(i_s)$, then a missing edge from $t \in \text{pre}(i_s)$ to i_s corresponds to the conditional independence relation $X_{i_s} \perp\!\!\!\perp X_t | \mathbb{X}_{\text{pre}(i_s) \setminus \{t\}}$. Given the result of the test hypothesis $\mathbf{H}_0 : \theta_{i_s t | \text{pre}(i_s) \cup \{i_s\}} = 0$, the set of parents of node i_s is defined as

$$\hat{p}a(i_s) = \{t \in \text{pre}(i_s) : \hat{\theta}_{i_s t | \text{pre}(i_s) \cup \{i_s\}} \neq 0\}.$$

It is worth to note that when \mathbf{p} is small (such as $\mathbf{p} = 10$), Or-LPGM performs similar to Or-PPGM while the average of the runtime of Or-PPGM is around 12 times that of Or-LPGM (see Supplementary, Table D.1). Hence, it is worth to consider this simple variant, Or-LPGM. However, when the number of variables is large (\mathbf{p} is large), the performance of Or-LPGM is overall less accurate than Or-PPGM. The reason for this difference is the difference between penalization and restriction of the conditional sets between the two algorithms. In the Or-PPGM algorithm, the number of variables in the conditional sets is controlled and progressively increased from 0 to $\mathbf{p} - 2$ (or to the stopping level m), see Nguyen and Chiogna (2021) for details.

4 | STATISTICAL GUARANTEES

In this section, we address the property of statistical consistency of Or-PPGM. In detail, we study the limiting behaviour of our estimation procedure as the sample size n , and the model size \mathbf{p} go to infinity. In what follows, we derive uniform consistency of our estimators explicitly as a function of the sample size, n , the number of nodes, \mathbf{p} , (and of m) by assuming that the true distribution is faithful to the graph. We acknowledge that our results are based on the work of Yang, Allen, Liu, and Ravikumar (2012) for exponential family models, combined with ideas coming from Kalisch and Bühlmann (2007).

For the readers' convenience, before stating the main result, we summarize some notation that will be used through out this proof. Given a vector $\mathbf{v} \in \mathbb{R}^{\mathbf{p}}$, and a parameter $q \in [0, \infty]$, we write $\|\mathbf{v}\|_q$ to denote the usual ℓ_q norm. Given a matrix $\mathbf{A} \in \mathbb{R}^{\mathbf{p} \times \mathbf{p}}$, denote the largest

and smallest eigenvalues as $\Lambda_{\max}(\mathbf{A})$, $\Lambda_{\min}(\mathbf{A})$, respectively. We use $\|\mathbf{A}\|_2 = \sqrt{\Lambda_{\max}(\mathbf{A}^T \mathbf{A})}$ to denote the spectral norm, corresponding to the largest singular value of \mathbf{A} , and the ℓ_∞ matrix norm is defined as $\|\mathbf{A}\|_\infty = \max_{i=1, \dots, a} \sum_{j=1}^a |A_{i,j}|$.

4.1 | Assumptions

We will begin by stating the assumptions that underlie our analysis, and then give a precise statement of the main results.

Denote the population Fisher information and the sample Fisher information matrix corresponding to the covariates in model (2) with $\mathbf{K} = \mathbf{V}$ as follows

$$I_s(\boldsymbol{\theta}_s) = -\mathbb{E}_{\boldsymbol{\theta}} \left(\nabla^2 \log \left(\mathbb{P}_{\boldsymbol{\theta}_s} (X_s | \mathbf{X}_{V \setminus \{s\}}) \right) \right),$$

and

$$Q_s(\boldsymbol{\theta}_s) = \nabla^2 \ell(\boldsymbol{\theta}_s, \mathbf{X}_s; \mathbf{X}_{V \setminus \{s\}}).$$

We note that we will consider the problem of maximum likelihood on a closed and bounded dish $\Theta \subset \mathbb{R}^{(p-1)}$. For $\boldsymbol{\theta}_{s|\mathbf{K}} \in \mathbb{R}^{|\mathbf{K}|-1}$, we can immerse $\boldsymbol{\theta}_{s|\mathbf{K}}$ into $\Theta \subset \mathbb{R}^{(p-1)}$ by zero-pad $\boldsymbol{\theta}_{s|\mathbf{K}}$ to include zero weights over $\{\mathbf{V} \setminus \mathbf{K}\}$.

Assumption 1. The coefficients $\boldsymbol{\theta}_{s|\mathbf{K}} \in \Theta$ for all sets $\mathbf{K} \subseteq \mathbf{V}$ and all $s \in \mathbf{K}$ have an upper bound norm, $\max_{s,t,\mathbf{K}} |\theta_{st|\mathbf{K}}| \leq M$, $\forall \theta_{st|\mathbf{K}} \neq 0$, and a lower bound norm, $\min_{s,t,\mathbf{K}} |\theta_{st|\mathbf{K}}| \geq c$, $\forall \theta_{st|\mathbf{K}} \neq 0$, where $t \in \mathbf{K}$.

Assumption 2. The Fisher information matrix corresponding to the covariates in model (2) with $\mathbf{K} = \mathbf{V}$ has bounded eigenvalues; that is, there exists a constant $\lambda_{\min} > 0$ such that

$$\Lambda_{\min}(I_s(\boldsymbol{\theta}_s)) \geq \lambda_{\min}, \forall \boldsymbol{\theta}_s \in \Theta.$$

Moreover, we require that

$$\Lambda_{\max} \left(\mathbb{E}_{\boldsymbol{\theta}} \left(\mathbf{X}_{V \setminus \{s\}}^T \mathbf{X}_{V \setminus \{s\}} \right) \right) \leq \lambda_{\max}, \forall s \in V, \forall \boldsymbol{\theta} \in \Theta,$$

where λ_{\max} is some constant such that $\lambda_{\max} < \infty$.

Remark 2. Assumption 1 simply bounds the effects of covariates in all local models. In other words, we consider parameters $\theta_{st|\mathbf{K}}$ belong to a compact set bounded by M . Being the expected value of the rescaled negative log-likelihood twice differentiable, the lower bound on the eigenvalues of the Fisher information matrix in Assumption 2 guarantees strong convexity in all partial models. Condition on the upper eigenvalue of the covariance matrix guarantees that the relevant covariates do not become overly dependent, a requirement which is commonly adopted in these settings.

Assumption 3. Suppose \mathbf{X} is a p -random vector with node conditional distribution specified in (2). Then, for any positive constant δ , there exists some constant $c_1 > 0$, such that

$$\mathbb{P}_{\boldsymbol{\theta}_s} (X_s \geq \delta \log n) \leq c_1 n^{-\delta}, \forall s \in V, \forall \boldsymbol{\theta}_s \in \Theta.$$

Assumption 4. Suppose \mathbf{X} is a p -random vector with node conditional distribution specified in (2). Then, for any $\boldsymbol{\theta} \in \Theta$, there exists some positive constants ν, c_2 , and $\gamma < 1/3$, such that

$$\mathbb{P}_{\boldsymbol{\theta}} (\nu + \langle \boldsymbol{\theta}, \mathbf{X} \rangle \geq \gamma \log n) \leq c_2 \kappa(n, \gamma),$$

where $\kappa(n, \gamma) = o_p(n^a)$ for some $a \leq -1$.

Remark 3. Condition on the marginal distribution in Assumption 3 guarantees that the considered variables do not have heavy tails, a common condition permitting to achieve consistency. Assumption 4 specifies the parameter space on which we are able to prove the consistency of local estimators.

Remark 4. Compared to Assumption 5 in Yang et al. (2012) and Condition 4 in Yang, Ravikumar, Allen, and Liu (2015), assumption 4 appears to be much weaker. Indeed, Yang et al. (2012) require $\gamma < \frac{1}{4}$ and $\|\boldsymbol{\theta}\|_2 \leq \frac{\log n}{18 \log(\max\{n, p\})}$, whereas we only require $\gamma < \frac{1}{3}$ and no specified bound is put on $\|\boldsymbol{\theta}\|_2$ (since the negative elements of $\boldsymbol{\theta}$ can be arbitrarily small). Moreover, Condition 4 in Yang et al. (2012) is written in analytical form, that is, a form more restrictive than the probability form here employed.

Remark 5. When conditional dependencies are all positive, a condition also known as ‘‘additive relationship’’ among variables, Assumption 4 also implies the sparsity of the graphs.

According to Lemma 1 in Ravikumar, Wainwright, and Lafferty (2010) and Lemma C.1 in Supplementary Material, Section C, the lower bound in Assumption 2 also guarantees uniqueness of the solution in the penalized setting.

4.2 | Consistency of the Or-PPGM algorithm

Theorem 1. Assume 1- 4. Denote by $\hat{G}(\alpha_n)$ the estimator resulting from Algorithm 1, and by G the true graph. Then, there exists a numerical sequence $\alpha_n \rightarrow 0$, such that

$$\mathbb{P}_{\theta}(\hat{G}(\alpha_n) = G) = 1, \forall \theta \in \Omega(\Theta),$$

when $n \rightarrow \infty$, where $\Omega(\Theta)$ is the space such that the faithfulness assumption is satisfied.

Proof. For different topological orderings T_1, T_2, \dots, T_k , Algorithm 1 performs sequences of tests S_1, S_2, \dots, S_k , respectively. We note that $S_j, j = 1, \dots, k$ is a subsequence of the sequence of tests performed in PC-LPGM Nguyen and Chiogna (2021). Hence, the proof of Theorem 4.1 in Nguyen and Chiogna (2021) shows that there exists a numerical sequence $\alpha_n \rightarrow 0$, such that, the estimators $\hat{G}^T(\alpha_n), T = T_1, T_2, \dots, T_k$ converge to the true graph. □

Remark 6. Different DAGs can encode the same set of conditional independences. Therefore, DAG models can be defined only up to their Markov equivalence class, a set of DAGs that have the same set of conditional independence. However, Poisson DAG models in (2) are identifiable, as we prove in Supplementary Material, Section A, benefiting from the ideas developed in the work of Peters and Bühlmann (2013), and avoiding a redundant condition in Park and Raskutti (2015) (see Theorem 3.1), who also recently provided a proof of identifiability. The property of identifiability has important consequences in our setting. Indeed, it guarantees that the true graph is unique, and, consequently, that Or-PPGM converges to the true unique graph irrespective of which ordering among the true existing ones is chosen to inform the algorithm.

5 | EMPIRICAL STUDY

Here, we empirically evaluate the ability of our proposal to retrieve the true DAG and compare them to a number of popular competitors. As measure of ability to recover the true structure of the graphs, we adopt three criteria including Precision P ; Recall R ; and their harmonic mean, known as F_1 -score, respectively defined as

$$P = \frac{TP}{TP + FP}, R = \frac{TP}{TP + FN}, F_1 = 2 \frac{P \cdot R}{P + R},$$

where TP (true positive), FP (false positive), and FN (false negative) refer to the number of inferred edges (Liu, Roeder, & Wasserman 2010).

As competitors, we consider structure learning algorithms for both Poisson and non Poisson variables. In detail, as representatives of algorithms for Poisson data, we consider: i) one variant of K2 algorithm (Cooper & Herskovits 1992), PKBIC, able to deal with Poisson data and based on a scoring criterion frequently used in model selection (see Supplementary Material, Section B for details); ii) the PDN algorithm in Hadiji et al. (2015); iii) the overdispersion scoring (ODS) algorithm in Park and Raskutti (2015). It is worth noting that PKBIC is indeed a new structure learning algorithm for Poisson data, whose consistency is proved in Supplementary Material, Section B. Moreover, we consider a structure learning method dealing with the class of categorical data, namely the Max Min Hill Climbing (MMHC) algorithm (Tsamardinos, Brown, & Aliferis 2006). To apply such algorithms, we categorize our data using the strategy: Gaussian mixture models on log transformed data shifted by 1 (Fraleigh & Raftery 2002). Finally, taking into account that structure learning for discrete data is usually performed by employing methods for continuous data after suitable data transformation, we consider one representative of approaches based on the Gaussian assumption, that is, the PC algorithm (Kalisch & Bühlmann 2007), applied to log transformed data shifted by 1.

5.1 | Data generation

For two different cardinalities, $p = 10$ and $p = 100$, we consider three graphs of different structure: (i) a scale-free graph; (ii) a hub graph; (iii) a random graph. See Figure 1 and 2 for a plot of the three chosen DAGs for $p = 10$ and $p = 100$, respectively.

In order to simulate data, we first construct an adjacency matrix $\text{Adj} = (\theta_{ij})$ as follows:

1. fill in the adjacency matrix Adj with zeros;
2. replace every entry corresponding to a directed edge by one;

3. replace each entry equal to 1 with an independent realization from a Uniform($[-0.5, 0.5]$) random variable, representing the true values of parameter θ_{st} .

This yields a matrix Adj whose entries are either zeros or in the range $[-0.5, 0.5]$, representing positive and negative relations among variables. For each DAG corresponding to an adjacency matrix Adj , 50 datasets are sampled for four sample sizes, $n = 100, 200, 500, 1000$ with $p = 10$, and $n = 200, 500, 1000, 2000$ with $p = 100$ as follows. The realization of the first random variable X_{i_1} in the topological ordering i_1, i_2, \dots, i_p is sampled from a $\text{Pois}(\exp\{\theta_1\})$, where the default value of θ_1 is 0. Realizations of the following random variables are recursively sampled from

$$X_{i_j}^{(t)} \sim \text{Pois}\left(\exp\left\{\sum_{k=i_1}^{i_{(j-1)}} \theta_{i_j k} x_{tk}\right\}\right).$$

5.2 | Learning algorithms

Acronyms of the considered algorithms are listed below, along with specifications, if needed, of tuning parameters. In this study, beside the topological ordering, we also specify an additional input, the upper limit for the cardinality of conditional sets, m , which in this study was set to $m = 8$ for $p = 10$ and $m = 3$ for $p = 100$, respectively.

- PKBIC: PK2 using BIC;
- Or-PPGM;
- Or-LPGM;
- PDN;
- ODS: k-fold cross validation ($k = 10$);
- MMHC: applied to data categorized by mixture models, using χ^2 tests of independence.
- PC: PC algorithm applied to log transformed data, using Gaussian conditional independent tests.

We note that ODS, PDN and MMHC employ a preliminary step aimed to estimate the topological ordering. This makes the comparison with our algorithms not completely fair. Nevertheless, we decided to consider these algorithms in our numerical studies to get a measure of impact of the knowledge of the true topological ordering.

It is also worth noting that the PC algorithm returns a PDAGs that consists of both directed and undirected edges. In this case, we borrow the idea of Dor and Tarsi (1992) to extend a PDAG to DAG. For details of the algorithm, we refer the interested reader to the paper by Dor and Tarsi (1992).

5.3 | Results

For the two considered vertex cardinalities, $p = 10, 100$, and for the chosen sample sizes, $n = 100, 200, 500, 1000, 2000$, Table 1 and Table 2 report, respectively, Monte Carlo means of TP, FP, FN, P, R and F_1 score for each of considered method. Each value is computed as an average of the 150 values obtained by simulating 50 samples for each of the three networks. Results disaggregated by network types are given in Supplementary Material, Section D, Tables D.1, and Tables D.2. These results indicate that the proposed algorithm, along with the modification of K2 (PKBIC) described in Supplementary Material, Section B, outperform, on average, Gaussian-based competitors (PC), category-based competitors (MMHC), as well as the state-of-the-art algorithms that are specifically designed for Poisson graphical models (ODS, PDN).

When $p = 10$, the algorithms PKBIC, Or-PPGM and Or-LPGM reach the highest F_1 score, followed by the ODS, and the PC algorithms. When $n \geq 1000$, the three first algorithms recover almost all edges, see Figure 3. A closer look at the Precision P and Recall R plot (see Figure D.1 in Supplementary, Section D.2) provides further insight into the behaviour of considered methods. The PKBIC, the Or-LPGM and the Or-PPGM algorithm always reach the highest Precision P and Recall R.

It is interesting to note that the performance of PKBIC, Or-PPGM and Or-LPGM appears to be far better than that of the competing algorithms employing the Poisson assumption (PDN and ODS). The use of the topological ordering overcomes the inaccuracies of the first step of the ODS algorithm, that is, identification of the order of variables, as well as the uncertainties in recovering the direction of interactions in PDN. On the other side, we also need to stress the good performances of Or-PPGM related to the difference between

penalization and restriction of the conditional sets. In the PDN algorithm, as well as in the ODS algorithm, a prediction model is fitted locally on all other variables, by means of a series of independent penalized regressions. In contrast, Or-PPGM controls the number of variables in the conditional sets for node s , which is progressively increased from 0 to $\min\{m, \text{ord}(s) - 1\}$.

When considering other methods, category-based methods (MMHC), and Gaussian-based method (PC), both perform less accurately. This result can be explained by the loss of information due to the data transformation. Moreover, this approach can be also ill-suited, possibly leading to wrong inferences in some circumstances (Gallopín, Rau, & Jaffrézic 2013).

Results for the high dimensional setting ($p = 100$) are somehow comparable to the ones of the previous setting, as it can be seen in Figures 4, and Figure D.2 in Supplementary, Section D.2. The performance of considered algorithms are classed into two different groups. In detail, PKBIC, Or-PPGM, and Or-LPGM still rank as the top three best algorithms, with Or-LPGM scoring as the best performing one for the highest sample size. Overall, their F_1 scores become already reasonable when n approaches 1000 observations.

As a final remark, we note that the performances of ODS is overall less accurate as expected. A reason for it is that ODS uses the LPGM model (Allen & Liu 2013) to search the candidate parent sets for each node. As a consequence, the performance of ODS is highly dependent on the result getting from LPGM algorithm. However, this result depends on the tuning of its parameters (β , γ , sth , etc). Here, we used the best combination of parameters that we managed to find in Nguyen and Chiogna (2021), i.e., $B = 50$, $n\lambda_{\text{bda}} = 20$, $\frac{\lambda_{\text{min}}}{\lambda_{\text{max}}} = 0.01$, $\gamma = 10^{-6}$, $\text{sth} = 0.6$, $\beta = 0.1$ for $p = 10$ and $\beta = 0.05$ for $p = 100$.

6 | RESULTS ON NON-SMALL CELL LUNG CANCER DATA

Here, we show an application of our proposed algorithm to the problem of learning gene interactions starting from gene expression measurements on a set of lung cancer cells.

Specifically, we aim at reconstructing the manually curated network in Figure 2c of Xue et al. (2020) from gene expression data, exploiting the topological ordering deriving from the non-small cell lung cancer pathway, as defined in KEGG (Kanehisa & Goto 2000), which is directly connected to the scope of the original analysis. The undirected graph corresponding to the selected pathway was obtained using the graphite package (Sales, Calura, Cavalieri, & Romualdi 2012).

Briefly, the data consist of gene expression measurements of individual cells by RNA sequencing, which yields discrete counts as a measure of the activity of each gene. We followed the filtering procedure described in the original publication, which leads to a total of $n = 5055$ cells (see Xue et al. 2020, for details).

Xue et al. (2020) identified 10 different clusters of cells based on their sensitivity to a treatment. We selected only the cells in clusters 1, 3, 4, 5, and 10 as described in Fig. 1 Xue et al. (2020). These clusters correspond to the cells that showed resistance to the treatment and are of particular biological interest.

The network in Figure 2c of Xue et al. (2020) presents a total of 11 genes, of which, only 7 have a topological ordering based on the non-small cell lung cancer pathway and hence further considered for the analysis. The topological ordering of the considered genes is based on the pathway network. However, gene CDKN1A is part of an unconnected component of the pathway and so we decided to put it at the end of the order.

We then applied the Or-PPGM algorithm, with a significance level of 1%, and the results are shown in Figure 5. By visually comparing our estimated DAG with the manually curated network of Xue et al. (2020), we confirm that our algorithm is able to reconstruct, from gene expression data alone, a biologically meaningful structure that confirms several known biological processes. For instance, Xue et al. (2020) showed with independent experiments that increased EGFR signal shifts KRAS into an active/drug-insensitive state, which ultimately restore tumor growth. This is consistent with KRAS being a descendant of EGFR. Moreover, it is well known that GRB2 mediates the EGF-dependent activation of guanine nucleotide exchange on Ras (Gale, Kaplan, Lowenstein, Schlessinger, & Bar-Sagi 1993). The fact that our algorithm reconstructs this known signaling pathway holds promise on novel biological insight that could be provided by inspecting other, lesser known, gene interactions.

7 | CONCLUSIONS AND REMARKS

We have considered structure learning of DAGs for count data in a scenario where we have knowledge of one possible topological ordering of the variables. We have proposed various guided structure learning algorithms that owe their attractiveness to the improvement in accuracy and the reduction of computational costs due to exploitation of the topological ordering, an ingredient that considerably reduces the search space. For the new proposals, we have shown that the estimators enjoy strong statistical guarantees under assumptions considerably

weaker than those employed in related works. Following the empirical comparison with a number of different approaches, our proposals appear to be promising algorithms as far as prediction accuracy is concerned.

An important side effect of our empirical study was shading some light on the effect of data transformation finalized to the use of structure learning under model specifications irrespective of the discrete nature of the data, such as those for continuous or categorical data. We have noticed that making the data continuous by log transformation is better than categorizing them when the PC algorithm is used and that mixture-based categorization is better than cut points-based categorization with K2. This is an important empirical conclusion that we draw from this study.

Overall, our exploration has consolidated avenues for learning DAGs, the properties and applications of which leave much room for future research. For example, the topological ordering may be misspecified, or only a partial order on the set of nodes might be specified due to a number of reasons. How to tackle these and other extensions of our setting is the core of our current research.

ACKNOWLEDGEMENTS

D.R. was supported by the National Cancer Institute of the National Institutes of Health [2U24CA180996]. This work was supported in part by CZF2019-002443 (D.R. and T.K.H.N.) from the Chan Zuckerberg Initiative DAF, an advised fund of Silicon Valley Community Foundation.

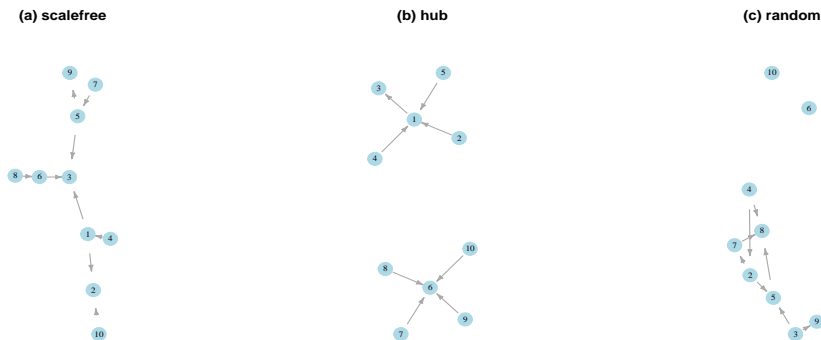


FIGURE 1 The graph structures for $p = 10$ employed in the simulation studies: (a) scale-free; (b) hub; (c) random graph.

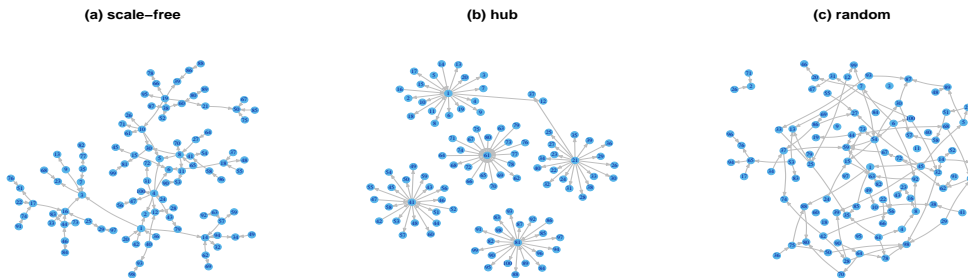


FIGURE 2 The graph structures for $p = 100$ employed in the simulation studies: (a) scale-free; (b) hub; (c) random graph.

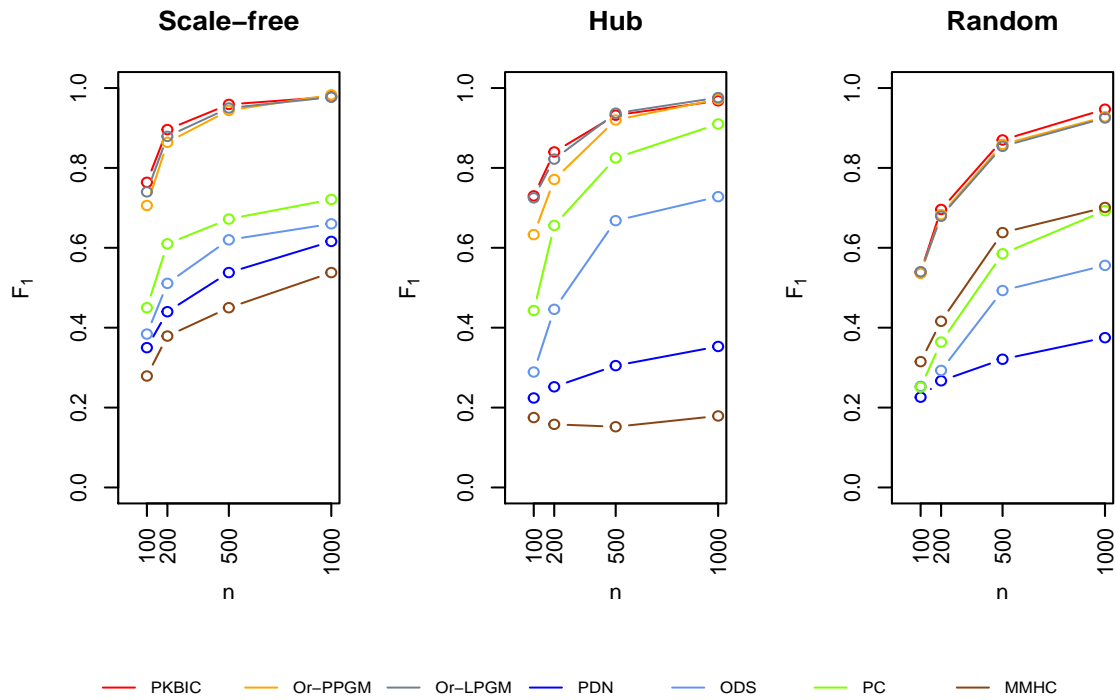


FIGURE 3 F_1 -score of the considered algorithms: PKBIC; Or-PPGM; Or-LPGM; PDN; ODS; MMHC; and PC for the three types of graphs in Figure 1 with $p = 10$ and sample sizes $n = 100, 200, 500, 1000$.

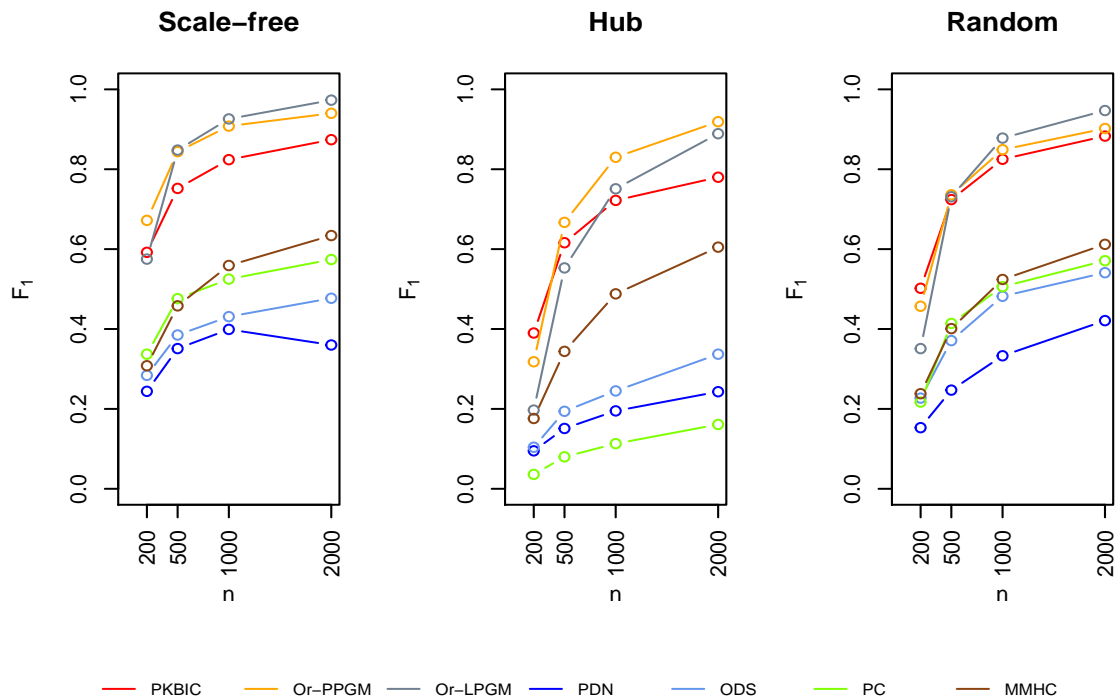


FIGURE 4 F_1 -score of the considered algorithms: PKBIC; Or-PPGM; Or-LPGM; PDN; ODS; MMHC; and PC for the three types of graphs in Figure 2 with $p = 100$ and sample sizes $n = 200, 500, 1000, 2000$.

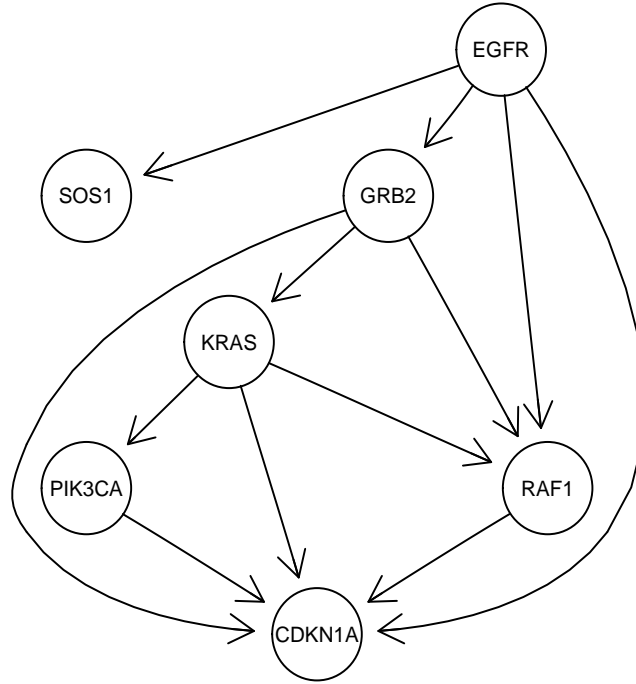


FIGURE 5 Non-small cell lung cancer network estimated by Or-PPGM algorithm.

TABLE 1 Monte Carlo marginal means of TP, FP, FN, P, R, and F_1 score obtained by simulating 50 samples from each of the three networks shown in Figure 1 ($\rho = 10$).

n	Algorithm	TP	FP	FN	P	R	F_1
100	PKBIC	5.133	1.393	3.200	0.791	0.613	0.678
	Or-PPGM	4.573	1.380	3.760	0.774	0.546	0.625
	Or-LPGM	5.200	1.740	3.133	0.758	0.621	0.669
	PDN	6.187	32.613	2.147	0.164	0.738	0.267
	ODS	1.791	0.721	6.581	0.786	0.211	0.315
	PC	2.734	2.604	5.626	0.511	0.325	0.392
	MMHC	1.723	3.088	6.635	0.381	0.205	0.260
	200	PKBIC	6.293	0.693	2.040	0.907	0.750
Or-PPGM		5.853	0.680	2.480	0.904	0.698	0.773
Or-LPGM		6.173	0.867	2.160	0.887	0.737	0.794
PDN		6.820	28.820	1.513	0.201	0.814	0.320
ODS		2.667	1.236	5.681	0.714	0.315	0.422
PC		4.062	2.000	4.283	0.654	0.484	0.550
MMHC		2.329	3.859	6.007	0.392	0.276	0.319
500		PKBIC	7.593	0.520	0.740	0.940	0.909
	Or-PPGM	7.340	0.433	0.993	0.947	0.879	0.907
	Or-LPGM	7.387	0.387	0.947	0.955	0.884	0.914
	PDN	7.067	22.180	1.267	0.258	0.844	0.388

TABLE 1 – continued from previous page

n	Algorithm	TP	FP	FN	P	R	F ₁
1000	ODS	4.347	1.813	3.987	0.714	0.520	0.593
	PC	5.450	1.839	2.886	0.746	0.654	0.694
	MMHC	3.338	4.365	5.000	0.444	0.398	0.417
	PKBIC	8.093	0.353	0.240	0.962	0.970	0.964
	Or-PPGM	7.907	0.180	0.427	0.979	0.948	0.961
	Or-LPGM	7.880	0.180	0.453	0.980	0.944	0.959
	PDN	7.307	17.927	1.027	0.309	0.873	0.448
	ODS	5.213	2.527	3.120	0.681	0.625	0.648
	PC	6.233	1.513	2.100	0.805	0.749	0.775
	MMHC	4.000	4.327	4.340	0.484	0.477	0.478

TABLE 2 Monte Carlo marginal means of TP, FP, FN, P, R, and F₁ score obtained by simulating 50 samples from each of the three networks shown in Figure 2 ($\rho = 100$).

n	Algorithm	TP	FP	FN	P	R	F ₁
200	PKBIC	60.220	81.113	40.780	0.424	0.595	0.495
	Or-PPGM	35.307	5.320	65.693	0.854	0.349	0.482
	Or-LPGM	26.107	6.340	74.893	0.780	0.258	0.374
	PDN	50.580	547.487	50.420	0.128	0.498	0.164
	ODS	23.413	91.947	77.587	0.201	0.229	0.205
	PC	14.399	16.601	86.895	0.403	0.141	0.205
	MMHC	27.527	98.873	73.473	0.216	0.272	0.241
	500	PKBIC	80.933	49.520	20.067	0.619	0.800
Or-PPGM	63.180	3.333	37.820	0.950	0.625	0.749	
Or-LPGM	58.813	2.493	42.187	0.956	0.580	0.711	
PDN	64.773	419.773	36.227	0.216	0.637	0.250	
ODS	36.040	84.007	64.960	0.298	0.353	0.317	
PC	26.693	26.127	74.307	0.444	0.259	0.323	
MMHC	47.993	89.340	53.007	0.348	0.474	0.401	
1000	PKBIC	89.000	34.685	12.013	0.719	0.879	0.790
	Or-PPGM	77.658	1.208	23.356	0.985	0.769	0.862
	Or-LPGM	76.153	0.200	24.847	0.997	0.751	0.852
	PDN	69.713	323.793	31.287	0.286	0.685	0.309
	ODS	45.413	83.947	55.587	0.355	0.444	0.386
	PC	34.087	32.827	66.913	0.459	0.331	0.381
	MMHC	62.447	74.787	38.553	0.455	0.618	0.524
	2000	PKBIC	91.833	23.713	9.167	0.794	0.906
Or-PPGM	87.273	1.493	13.727	0.984	0.865	0.920	
Or-LPGM	89.267	0.020	11.733	1.000	0.882	0.936	
PDN	67.733	237.620	33.267	0.338	0.664	0.341	
ODS	54.767	82.687	46.233	0.398	0.538	0.452	
PC	41.400	39.180	59.600	0.478	0.402	0.435	

TABLE 2 – continued from previous page

n	Algorithm	TP	FP	FN	P	R	F ₁
	MMHC	72.100	60.813	28.900	0.544	0.714	0.617



APPENDIX

A IDENTIFIABILITY

In what follows, we provide a proof of identifiability of models specified in Section 2 of the main paper.

Proposition A.1. Let \mathbf{X} be a \mathfrak{p} -random vector defined as in (2) and $G = (V, E)$ be a DAG. Consider a variable X_j , $j \in V$, and one of its parents $k \in \text{pa}_G(j)$. For all set S with $\text{pa}_G(j) \setminus \{k\} \subseteq S \subseteq \text{nd}_G(j) \setminus \{k\}$, we have $X_j \not\perp\!\!\!\perp X_k | \mathbf{X}_S$.

Proof. This proposition can be proved easily by using the definition of d-connection and the faithfulness assumption. Indeed, for a fixed node $j \in V$, for all $k \in \text{pa}_G(j)$ and for all set S satisfies $\text{pa}_G(j) \setminus \{k\} \subseteq S \subseteq \text{nd}_G(j) \setminus \{k\}$, there always exists the path $k \rightarrow j$ satisfies the definition of d-connection. Hence, $X_j \not\perp\!\!\!\perp X_k | \mathbf{X}_S$. \square

Theorem 1. The Poisson DAG model defined as in (2) is identifiable.

Proof. Assume there are two structure models as in (2) which both encode the same set of conditional independences, one with graph G , and the other with graph G' . We will show that $G \equiv G'$.

Since DAGs do not contain any cycles, we can always find one node without any child. Indeed, assume to start at some node, and follow a directed path that contains the chosen node. After at most $|V| - 1$ steps, a node without any child is reached. Eliminating such a node from the graph leads to a new DAG.

We repeat this process on G and G' for all nodes that have: (i) no children, (ii) the same parents in G and G' . This process terminates with one of two possible outputs: (a) no nodes left; (b) a subset of variables, which we call again \mathbf{X} , two sub-graphs, which we call again G and G' , and a node j that has no children in G such that either $\text{pa}_G(j) \neq \text{pa}_{G'}(j)$ or $\text{ch}_{G'}(j) \neq \emptyset$. If (a) occurs, the two graphs are identical and the result is proved. In what follows, we consider the case that (b) occurs.

For such a j node, we have

$$X_j \perp\!\!\!\perp X_{V \setminus (\text{pa}_{G'}(j) \cup \{j\})} | \mathbf{X}_{\text{pa}_{G'}(j)}, \quad (\text{A1})$$

thanks to the Markov properties with respect to G . To make our argument clear, we divide the set of parents $\text{pa}_G(j)$ into three disjoint partitions W, Y, Z representing, respectively, the set of common parents in both graphs; the set of parents in G being a subset of children in G' ; the set of parents in G which are not parents in G' . Formalizing,

- $Z = \text{pa}_G(j) \cap \text{pa}_{G'}(j)$;
- $Y \subset \text{pa}_G(j)$ such that $\text{ch}_{G'}(j) = Y \cup T$;
- $W \subset \text{pa}_G(j)$ such that W are not adjacent to j in G' .

Thus,

$$\begin{aligned} \text{pa}_G(j) &= W \cup Y \cup Z, & \text{ch}_G(j) &= \emptyset, \\ \text{pa}_{G'}(j) &= D \cup Z, & \text{ch}_{G'}(j) &= T \cup Y, \end{aligned}$$

where D is not adjacent to j in G . Let $U = W \cup Y$ and consider the following two cases:

- $U = \emptyset$. Then, there exists a node $d \in D$ or a node $t \in T$, otherwise j would have been discarded.
 - If there exists a node $d \in D$, (A1) implies $X_j \perp\!\!\!\perp X_d | \mathbf{X}_Q$, for $Q = Z \cup D \setminus \{d\}$, which contradicts Proposition (A.1) applied to G' .
 - If $D = \{\emptyset\}$, and there exists a node $t \in T$, then (A1) implies $X_j \perp\!\!\!\perp X_t | \mathbf{X}_Q$, for $Q = Z \cup \text{pa}_{G'}(t) \setminus \{j\}$, which contradicts Proposition (A.1) applied to G' .
- $U \neq \emptyset$. We note that, within the structure of the graph G' , the Poisson assumption implies

$$\text{Var}(X_j | \mathbf{X}_{\text{pa}_{G'}(j)}) = \mathbb{E}(X_j | \mathbf{X}_{\text{pa}_{G'}(j)}). \quad (\text{A2})$$

However, by applying the law of total variance we get

$$\begin{aligned} \text{Var}(X_j | \mathbf{X}_{\text{pa}_{G'}(j)}) &= \text{Var}(\mathbb{E}(X_j | \mathbf{X}_{\text{pa}_{G'}(j)} \cup \mathbf{X}_{\text{pa}_G(j)}) | \mathbf{X}_{\text{pa}_{G'}(j)}) \\ &\quad + \mathbb{E}(\text{Var}(X_j | \mathbf{X}_{\text{pa}_{G'}(j)} \cup \mathbf{X}_{\text{pa}_G(j)}) | \mathbf{X}_{\text{pa}_{G'}(j)}). \end{aligned}$$

By applying Property (A1) we can rewrite

$$\text{Var}(X_j | \mathbf{X}_{\text{pa}_{G'}(j)}) = \text{Var}(\mathbb{E}(X_j | \mathbf{X}_{\text{pa}_G(j)}) | \mathbf{X}_{\text{pa}_{G'}(j)}) + \mathbb{E}(\text{Var}(X_j | \mathbf{X}_{\text{pa}_G(j)}) | \mathbf{X}_{\text{pa}_{G'}(j)}). \quad (\text{A3})$$

Let $\mathbf{f}_s(\mathbf{X}_{\text{pa}(s)}) = \exp\{\sum_{t \in \text{pa}(s)} \theta_{st} X_t\}$, $\forall s \in \mathcal{V}$. In graph \mathbf{G} , we have $X_j | \mathbf{X}_{\text{pa}_G(j)} \sim \text{Pois}(f_j(\mathbf{X}_{\text{pa}_G(j)}))$, so that

$$\mathbb{E}(X_j | \mathbf{X}_{\text{pa}_G(j)}) = \text{Var}(X_j | \mathbf{X}_{\text{pa}_G(j)}) = f_j(\mathbf{X}_{\text{pa}_G(j)}).$$

Hence, from Equation (A3), we get

$$\begin{aligned} \text{Var}(X_j | \mathbf{X}_{\text{pa}_{G'}(j)}) &= \text{Var}(f_j(\mathbf{X}_{\text{pa}_G(j)}) | \mathbf{X}_{\text{pa}_{G'}(j)}) + \mathbb{E}(\mathbb{E}(X_j | \mathbf{X}_{\text{pa}_G(j)}) | \mathbf{X}_{\text{pa}_{G'}(j)}) \\ &= \text{Var}(f_j(\mathbf{X}_{\text{pa}_G(j)}) | \mathbf{X}_{\text{pa}_{G'}(j)}) + \mathbb{E}(\mathbb{E}(X_j | \mathbf{X}_{\text{pa}_G(j)} \cup \mathbf{X}_{\text{pa}_{G'}(j)}) | \mathbf{X}_{\text{pa}_{G'}(j)}) \\ &= \text{Var}(f_j(\mathbf{X}_{\text{pa}_G(j)}) | \mathbf{X}_{\text{pa}_{G'}(j)}) + \mathbb{E}(X_j | \mathbf{X}_{\text{pa}_{G'}(j)}), \end{aligned} \quad (\text{A4})$$

by applying (A1). Equation (A4) implies

$$\text{Var}(X_j | \mathbf{X}_{\text{pa}_{G'}(j)}) > \mathbb{E}(X_j | \mathbf{X}_{\text{pa}_{G'}(j)}),$$

since $\text{Var}(f_j(\mathbf{X}_{\text{pa}_G(j)}) | \mathbf{X}_{\text{pa}_{G'}(j)}) > 0$ in general, except at the root node. □

B THE PK2 ALGORITHM

K2 (Cooper & Herskovits 1992) is a structure learning algorithm which owes its popularity to its computational efficiency and simplicity. Technically speaking, it is defined only for categorical variables; a natural choice for using K2 on non-categorical data is categorization, a choice that highly depends on the algorithm chosen to categorize. In our empirical study, we develop a modification of K2, named PK2, that substitutes the K2 score with an alternative scoring criterion respectful of the nature of the data.

As alternative scoring criteria, we consider the Bayesian information criterion (BIC) (Schwarz 1978) and the Akaike information criterion (AIC) (Akaike 1974), that both balance goodness of fit and model parsimony. PK2 works in two steps: (i) forward phase, and (ii) backward phase. In the forward phase, we employ the same search strategy as in the K2 algorithm. Then, the result from the first phase is taken as the input of the second phase. Here, we use the score to prune the estimated graph by deleting edges that gain larger scores.

The asymptotic property of PK2 is proved by results of ?, that states that under the assumption of a generative distribution perfect w.r.t. the structure from which the data was generated, the greedy search identifies the true structure up to an equivalent class as the number of observations goes to infinity when a consistent scoring criterion is used.

As both BIC and AIC are consistent scoring criteria (Haughton et al. 1988), and the perfect property is guaranteed by Markov and Faithfulness assumption, Lemma 10 of ? holds for PK2. Moreover, the Poisson model is identifiable (see Appendix A). Therefore, the estimator in PK2 algorithm converges asymptotically to the true graph.

We note that PKAIC (PK2 using AIC) usually performs more poorly than the PKBIC (PK2 using BIC). This result is not surprising since the PKAIC using the AIC criterion penalizes less strongly than the BIC one. As a consequence, the PKAIC results in graphs with more edges than PKBIC does, see Wagenmakers and Farrell (2004). For this reason, we consider only PKBIC in the main paper.

C PROOFS

Here, we provide proofs of results needed to show consistency of our algorithms. These results are central for both OR-LPGM and OR-PPGM. They are presented in a form tailored on Or-PPGM. The adaptation to the Or-LPGM setting follows by substituting δ with $\delta(\lambda)$.

Before going into details, we first prove the following Lemma, used in the proof of Theorem 2.

Lemma C.1. Assume 2 - 5. Then, for any $\delta > 0$, we have

$$\begin{aligned} \mathbb{P}_{\boldsymbol{\theta}} \left(\Lambda_{\max} \left(\frac{1}{n} \sum_{i=1}^n (\mathbf{X}_{V \setminus \{s\}}^{(i)})^T \mathbf{X}_{V \setminus \{s\}}^{(i)} \right) \leq \lambda_{\max} + \delta \right) &\geq 1 - \exp \left\{ -c'_1 \frac{\delta^2 n}{p^2 n^{2\gamma} \log^4 n} + c'_2 \log p \right\} \\ &\quad - c_2 n \kappa(n, \gamma) - c_1 n^{-2} \\ \mathbb{P}_{\boldsymbol{\theta}} (\Lambda_{\min} (\mathbf{Q}_s(\boldsymbol{\theta}_s)) \geq \lambda_{\min} - \delta) &\geq 1 - \exp \left\{ -c'_1 \frac{\delta^2 n}{p^2 n^{2\gamma} \log^4 n} + c'_2 \log p \right\} \\ &\quad - c_2 n \kappa(n, \gamma) - c_1 n^{-2}. \end{aligned}$$

Proof. We have

$$\begin{aligned} \Lambda_{\min}(\mathbf{I}_s(\boldsymbol{\theta}_s)) &= \min_{\|\mathbf{y}\|_2=1} \mathbf{y}^T \mathbf{I}_s(\boldsymbol{\theta}_s) \mathbf{y} \\ &= \min_{\|\mathbf{y}\|_2=1} \left\{ \mathbf{y}^T \mathbf{Q}_s(\boldsymbol{\theta}_s) \mathbf{y} + \mathbf{y}^T (\mathbf{I}_s(\boldsymbol{\theta}_s) - \mathbf{Q}_s(\boldsymbol{\theta}_s)) \mathbf{y} \right\} \\ &\leq \lambda_{\min}(\mathbf{Q}_s(\boldsymbol{\theta}_s)) + \max_{\|\mathbf{y}\|_2=1} \mathbf{y}^T (\mathbf{I}_s(\boldsymbol{\theta}_s) - \mathbf{Q}_s(\boldsymbol{\theta}_s)) \mathbf{y}, \end{aligned}$$

where $\mathbf{y} \in \mathbb{R}^{p-1}$ is an arbitrary vector with unit norm. Hence,

$$\Lambda_{\min}(\mathbf{Q}_s(\boldsymbol{\theta}_s)) \geq \Lambda_{\min}(\mathbf{I}_s(\boldsymbol{\theta}_s)) - \max_{\|\mathbf{y}\|_2=1} \mathbf{y}^T (\mathbf{I}_s(\boldsymbol{\theta}_s) - \mathbf{Q}_s(\boldsymbol{\theta}_s)) \mathbf{y} \geq \lambda_{\min} - \|\mathbf{I}_s(\boldsymbol{\theta}_s) - \mathbf{Q}_s(\boldsymbol{\theta}_s)\|_2. \quad (\text{C5})$$

It remains to control the spectral norm $\|\mathbf{I}_s(\boldsymbol{\theta}_s) - \mathbf{Q}_s(\boldsymbol{\theta}_s)\|_2$. The (j, k) element of the matrix $\mathbf{Z}^n = \mathbf{Q}_s(\boldsymbol{\theta}_s) - \mathbf{I}_s(\boldsymbol{\theta}_s)$ can be written as

$$\begin{aligned} Z_{jk}^n(\boldsymbol{\theta}_s) &= \frac{1}{n} \sum_{i=1}^n D(\langle \boldsymbol{\theta}_s, \mathbf{X}_{V \setminus \{s\}}^{(i)} \rangle) X_{ij} X_{ik} - \mathbb{E}_{\boldsymbol{\theta}} (D(\langle \boldsymbol{\theta}_s, \mathbf{X}_{V \setminus \{s\}} \rangle) X_j X_k) \\ &= \frac{1}{n} \sum_{i=1}^n Y_i - \mathbb{E}_{\boldsymbol{\theta}} \left(\frac{1}{n} \sum_{i=1}^n Y_i \right), \end{aligned}$$

where $Y_i = D(\langle \boldsymbol{\theta}_s, \mathbf{X}_{V \setminus \{s\}}^{(i)} \rangle) X_{ij} X_{ik}$, $i = 1, \dots, n$ are independent.

Let $\zeta_1 = \{\max_i X_{it} < 3 \log n\}$, and $\zeta_4 = \{\max_i \langle \boldsymbol{\theta}_s, \mathbf{X}_{V \setminus \{s\}}^{(i)} \rangle < \gamma \log n\}$. From Assumption 4, we get

$$\mathbb{P}_{\boldsymbol{\theta}}(\zeta_1^c) \leq c_1 n n^{-3} = c_1 n^{-2}.$$

Moreover, by Assumption 5, we have

$$\begin{aligned} \mathbb{P}_{\boldsymbol{\theta}}(\zeta_4^c) &= \mathbb{P}_{\boldsymbol{\theta}}(\max_i \langle \boldsymbol{\theta}_s, \mathbf{X}_{V \setminus \{s\}}^{(i)} \rangle \geq \gamma \log n) \\ &= \mathbb{P}_{\boldsymbol{\theta}}(\max_i \langle \boldsymbol{\theta}_s, \mathbf{X}_{V \setminus \{s\}}^{(i)} \rangle \geq \gamma \log n, \zeta_1) + \mathbb{P}_{\boldsymbol{\theta}}(\max_i \langle \boldsymbol{\theta}_s, \mathbf{X}_{V \setminus \{s\}}^{(i)} \rangle \geq \gamma \log n, \zeta_1^c) \\ &\leq n \mathbb{P}_{\boldsymbol{\theta}}(\langle \boldsymbol{\theta}_s, \mathbf{X}_{V \setminus \{s\}}^{(i)} \rangle \geq \gamma \log n, \zeta_1) + \mathbb{P}_{\boldsymbol{\theta}}(\zeta_1^c) \\ &\leq n \mathbb{P}_{\boldsymbol{\theta}}(\nu + \langle \boldsymbol{\theta}_s, \mathbf{X}_{V \setminus \{s\}}^{(i)} \rangle \geq \gamma \log n) + \mathbb{P}_{\boldsymbol{\theta}}(\zeta_1^c) \\ &\leq c_2 n \kappa(n, \gamma) + c_1 n^{-2}. \end{aligned}$$

Conditioning on ζ_1, ζ_4 , we get

$$|Y_i| \leq 9n^\gamma \log^2 n.$$

Then, by the Azuma-Hoeffding inequality (Theorem 2 in Hoeffding 1963), for any $\epsilon > 0$, we obtain

$$\mathbb{P}_{\boldsymbol{\theta}} \left((Z_{ij}^n)^2 \geq \epsilon^2 | \zeta_1, \zeta_4 \right) = \mathbb{P}_{\boldsymbol{\theta}} \left(|Z_{ij}^n| \geq \epsilon | \zeta_1, \zeta_4 \right) \leq 2 \exp \left(-\frac{\epsilon^2 n}{18n^{2\gamma} \log^4 n} \right).$$

Let $\epsilon = \delta/p$, then

$$\begin{aligned} \mathbb{P}_{\boldsymbol{\theta}} (\|\mathbf{I}_s(\boldsymbol{\theta}_s) - \mathbf{Q}_s(\boldsymbol{\theta}_s)\|_2 \geq \delta) &\leq \mathbb{P}_{\boldsymbol{\theta}} \left(\left(\sum_{j,k \neq s} (Z_{jk}^n)^2 \right)^{1/2} \geq \delta \right) \\ &\leq \mathbb{P}_{\boldsymbol{\theta}} \left(\left(\sum_{j,k \neq s} (Z_{jk}^n)^2 \right)^{1/2} \geq \delta | \zeta_1, \zeta_4 \right) + \mathbb{P}_{\boldsymbol{\theta}}(\zeta_4^c) + \mathbb{P}_{\boldsymbol{\theta}}(\zeta_1^c) \\ &\leq 2p^2 \exp \left\{ -\frac{\delta^2 n}{18p^2 n^{2\gamma} \log^4 n} \right\} + c_2 n \kappa(n, \gamma) + c_1 n^{-2} \\ &\leq \exp \left\{ -c'_1 \frac{\delta^2 n}{p^2 n^{2\gamma} \log^4 n} + c'_2 \log p \right\} + c_2 n \kappa(n, \gamma) + c_1 n^{-2}. \end{aligned} \quad (\text{C6})$$

From Equation (C5) and (C6), we have

$$\mathbb{P}_{\boldsymbol{\theta}} (\Lambda_{\min}(\mathbf{Q}_s(\boldsymbol{\theta}_s)) \geq \lambda_{\min} - \delta) \geq 1 - \exp \left\{ -c'_1 \frac{\delta^2 n}{p^2 n^{2\gamma} \log^4 n} + c'_2 \log p \right\} - c_2 n \kappa(n, \gamma) - c_1 n^{-2}.$$

Similarly,

$$\mathbb{P}_{\boldsymbol{\theta}} \left(\Lambda_{\max} \left[\frac{1}{n} \sum_{i=1}^n (\mathbf{X}_{V \setminus \{s\}}^{(i)})^T \mathbf{X}_{V \setminus \{s\}}^{(i)} \right] \leq \lambda_{\max} + \delta \right) \geq 1 - \exp \left\{ -c'_1 \frac{\delta^2 n}{p^2 n^2 \gamma \log^4 n} + c'_2 \log p \right\} - c_2 n \kappa(n, \gamma) - c_1 n^{-2}.$$

□

Proposition C.2. Assume 1- 5. Then, for any $\delta > 0$

$$\mathbb{P}_{\boldsymbol{\theta}} (\|\nabla l(\boldsymbol{\theta}_s, \mathbf{X}_s; \mathbf{X}_{V \setminus \{s\}})\|_{\infty} \geq \delta) \leq \exp(-c_3 n) + c_2 n \kappa(n, \gamma) + c_1 n^{-2}, \quad \forall \boldsymbol{\theta} \in \Theta,$$

when $n \rightarrow \infty$.

Proof. The t -partial derivative of the node conditional log-likelihood $l(\boldsymbol{\theta}_s, \mathbf{X}_s; \mathbf{X}_{V \setminus \{s\}})$ is:

$$\mathbf{W}_t = \nabla_t l(\boldsymbol{\theta}_s, \mathbf{X}_s; \mathbf{X}_{V \setminus \{s\}}) = \frac{1}{n} \sum_{i=1}^n \left[-X_{is} X_{it} + X_{it} D(\langle \boldsymbol{\theta}_s, \mathbf{X}_{V \setminus \{s\}}^{(i)} \rangle) \right]$$

Let $V_{is}(t) = X_{is} X_{it} - X_{it} D(\langle \boldsymbol{\theta}_s, \mathbf{X}_{V \setminus \{s\}}^{(i)} \rangle)$. We have,

$$\begin{aligned} \mathbb{P}_{\boldsymbol{\theta}} (\|\mathbf{W}\|_{\infty} > \delta) &= \mathbb{P}_{\boldsymbol{\theta}} \left(\max_{t \in V \setminus \{s\}} |\nabla_t l(\boldsymbol{\theta}_s, \mathbf{X}_s, \mathbf{X}_{V \setminus \{s\}})| > \delta \right) \\ &\leq \mathbb{P}_{\boldsymbol{\theta}} \left(\max_{t \in V \setminus \{s\}} \left| \frac{1}{n} \sum_{i=1}^n V_{is}(t) \right| > \delta | \zeta_1, \zeta_2 \right) + \mathbb{P}_{\boldsymbol{\theta}}(\zeta_1^c) + \mathbb{P}_{\boldsymbol{\theta}}(\zeta_2^c) \\ &\leq p \left[\mathbb{P}_{\boldsymbol{\theta}} \left(\frac{1}{n} \sum_{i=1}^n V_{is}(t) > \delta | \zeta_1, \zeta_2 \right) + \mathbb{P}_{\boldsymbol{\theta}} \left(-\frac{1}{n} \sum_{i=1}^n V_{is}(t) > \delta | \zeta_1, \zeta_2 \right) \right] \\ &\quad + \mathbb{P}_{\boldsymbol{\theta}}(\zeta_1^c) + \mathbb{P}_{\boldsymbol{\theta}}(\zeta_2^c) \\ &\leq p \left[\frac{\mathbb{E}_{\boldsymbol{\theta}} \left[\prod_{i=1}^n \exp(h V_{is}(t)) | \zeta_1, \zeta_2 \right]}{\exp(nh\delta)} + \frac{\mathbb{E}_{\boldsymbol{\theta}} \left[\prod_{i=1}^n \exp(-h V_{is}(t)) | \zeta_1, \zeta_2 \right]}{\exp(nh\delta)} \right] \\ &\quad + \mathbb{P}_{\boldsymbol{\theta}}(\zeta_1^c) + \mathbb{P}_{\boldsymbol{\theta}}(\zeta_2^c) \\ &= p \left[\frac{\prod_{i=1}^n \mathbb{E}_{\boldsymbol{\theta}} [\exp(h V_{is}(t)) | \zeta_1, \zeta_2]}{\exp(nh\delta)} + \frac{\prod_{i=1}^n \mathbb{E}_{\boldsymbol{\theta}} [\exp(-h V_{is}(t)) | \zeta_1, \zeta_2]}{\exp(nh\delta)} \right] \\ &\quad + \mathbb{P}_{\boldsymbol{\theta}}(\zeta_1^c) + \mathbb{P}_{\boldsymbol{\theta}}(\zeta_2^c) \\ &= p \left[\exp \left\{ \sum_{i=1}^n \log \mathbb{E}_{\boldsymbol{\theta}} [\exp(h V_{is}(t)) | \zeta_1, \zeta_2] - nh\delta \right\} \right. \\ &\quad \left. + \exp \left\{ \sum_{i=1}^n \log \mathbb{E}_{\boldsymbol{\theta}} [\exp(-h V_{is}(t)) | \zeta_1, \zeta_2] - nh\delta \right\} \right] + \mathbb{P}_{\boldsymbol{\theta}}(\zeta_1^c) + \mathbb{P}_{\boldsymbol{\theta}}(\zeta_2^c), \end{aligned} \tag{C7}$$

for some $h > 0$, where $\zeta_1 = \{\max_i X_{it} < 3 \log n\}$, $\zeta_2 = \{\max_i (v_h X_{it} + \langle \boldsymbol{\theta}_s, \mathbf{X}_{V \setminus \{s\}}^{(i)} \rangle) < \gamma \log n\}$. From Lemma C.1, we have $\mathbb{P}_{\boldsymbol{\theta}}(\zeta_1^c) \leq c_1 n^{-2}$.

Compute ζ_2 similarly to ζ_4 in Lemma C.1, we get

$$\begin{aligned} \mathbb{P}_{\boldsymbol{\theta}}(\zeta_2^c) &= \mathbb{P}_{\boldsymbol{\theta}} \left(\max_i (v_h X_{it} + \langle \boldsymbol{\theta}_s, \mathbf{X}_{V \setminus \{s\}}^{(i)} \rangle) \geq \gamma \log n \right) \\ &\leq \mathbb{P}_{\boldsymbol{\theta}} \left(\max_i (v_h X_{it} + \langle \boldsymbol{\theta}_s, \mathbf{X}_{V \setminus \{s\}}^{(i)} \rangle) \geq \gamma \log n, \zeta_1 \right) + \mathbb{P}_{\boldsymbol{\theta}}(\zeta_1^c) \\ &\leq \mathbb{P}_{\boldsymbol{\theta}} \left(\max_i (\nu + \langle \boldsymbol{\theta}_s, \mathbf{X}_{V \setminus \{s\}}^{(i)} \rangle) \geq \gamma \log n, \zeta_1 \right) + \mathbb{P}_{\boldsymbol{\theta}}(\zeta_1^c) \\ &\leq c_2 n \kappa(n, \gamma) + c_1 n^{-2}, \end{aligned}$$

provided that $|h| < \frac{\nu}{3 \log n}$. We therefore need to compute $\sum_{i=1}^n \log \mathbb{E}_{\boldsymbol{\theta}} [\exp(\mathbf{hV}_{is}(t)) | \zeta_1, \zeta_2]$, and $\sum_{i=1}^n \log \mathbb{E}_{\boldsymbol{\theta}} [\exp(-\mathbf{hV}_{is}(t)) | \zeta_1, \zeta_2]$. First, we have

$$\begin{aligned} \mathbb{E}_{\boldsymbol{\theta}_s} \left[\exp(\mathbf{hV}_{is}(t)) | \mathbf{x}_{V \setminus \{s\}}^{(i)} \right] &= \sum_{x_{is}=0}^{\infty} \exp \left\{ h[x_{is}x_{it} - x_{it}D(\langle \boldsymbol{\theta}_s, \mathbf{x}_{V \setminus \{s\}}^{(i)} \rangle)] \right. \\ &\quad \left. + x_{is} \langle \boldsymbol{\theta}_s, \mathbf{x}_{V \setminus \{s\}}^{(i)} \rangle - \log x_{is}! - D(\langle \boldsymbol{\theta}_s, \mathbf{x}_{V \setminus \{s\}}^{(i)} \rangle) \right\} \\ &= \sum_{x_{is}=0}^{\infty} \exp \left\{ x_{is} [hx_{it} + \langle \boldsymbol{\theta}_s, \mathbf{x}_{V \setminus \{s\}}^{(i)} \rangle] - \log x_{is}! \right. \\ &\quad \left. - hx_{it}D(\langle \boldsymbol{\theta}_s, \mathbf{x}_{V \setminus \{s\}}^{(i)} \rangle) - D(\langle \boldsymbol{\theta}_s, \mathbf{x}_{V \setminus \{s\}}^{(i)} \rangle) \right\} \\ &= \exp \left\{ D(hx_{it} + \langle \boldsymbol{\theta}_s, \mathbf{x}_{V \setminus \{s\}}^{(i)} \rangle) - D(\langle \boldsymbol{\theta}_s, \mathbf{x}_{V \setminus \{s\}}^{(i)} \rangle) \right. \\ &\quad \left. - hx_{it}D(\langle \boldsymbol{\theta}_s, \mathbf{x}_{V \setminus \{s\}}^{(i)} \rangle) \right\} \\ &= \exp \left\{ \frac{h^2}{2} (x_{it})^2 D(vhx_{it} + \langle \boldsymbol{\theta}_s, \mathbf{x}_{V \setminus \{s\}}^{(i)} \rangle) \right\}, \end{aligned}$$

for some $\nu \in [0, 1]$, where we move from line 2 to line 3 by applying $e^\lambda = \sum_{x=0}^{\infty} \frac{e^x}{x!}$, and from line 3 to line 4 by using a Taylor expansion for function $D(\cdot)$ at $\langle \boldsymbol{\theta}_s, \mathbf{x}_{V \setminus \{s\}}^{(i)} \rangle$. Therefore,

$$\sum_{i=1}^n \log \mathbb{E}_{\boldsymbol{\theta}} [\exp(\mathbf{hV}_{is}(t)) | \zeta_1, \zeta_2] \tag{C8}$$

$$\begin{aligned} &= \sum_{i=1}^n \log \mathbb{E}_{\boldsymbol{\theta}_{V \setminus \{s\}}} \left[\mathbb{E}_{\boldsymbol{\theta}_s} \left[\exp(\mathbf{hV}_{is}(t)) | \mathbf{x}_{V \setminus \{s\}}^{(i)} \right] | \zeta_1, \zeta_2 \right] \\ &= \sum_{i=1}^n \log \mathbb{E}_{\boldsymbol{\theta}_{V \setminus \{s\}}} \left[\exp \left\{ \frac{h^2}{2} (X_{it})^2 D(vhX_{it} + \langle \boldsymbol{\theta}_s, \mathbf{X}_{V \setminus \{s\}}^{(i)} \rangle) \right\} | \zeta_1, \zeta_2 \right] \\ &\leq \sum_{i=1}^n \log \mathbb{E}_{\boldsymbol{\theta}_{V \setminus \{s\}}} \left[\exp \left\{ \frac{h^2}{2} (3 \log n)^2 D(\gamma \log n) \right\} | \zeta_1, \zeta_2 \right] \\ &= n \left\{ \frac{h^2}{2} (3 \log n)^2 n^\gamma \right\} \end{aligned} \tag{C9}$$

Similarly,

$$\mathbb{E}_{\boldsymbol{\theta}_s} \left[\exp(-\mathbf{hV}_{is}(t)) | \mathbf{x}_{V \setminus \{s\}}^{(i)} \right] = \exp \left\{ \frac{h^2}{2} (x_{it})^2 D(-vhx_{it} + \langle \boldsymbol{\theta}_s, \mathbf{x}_{V \setminus \{s\}}^{(i)} \rangle) \right\}.$$

Hence,

$$\sum_{i=1}^n \log \mathbb{E}_{\boldsymbol{\theta}} [\exp(-\mathbf{hV}_{is}(t)) | \zeta_1, \zeta_2] \leq n \left\{ \frac{h^2}{2} (3 \log n)^2 n^\gamma \right\} \tag{C10}$$

Let $h = \frac{\delta}{9n^\gamma \log^2 n}$, from (C7)–(C10), we get

$$\begin{aligned} \mathbb{P}_{\boldsymbol{\theta}} (\|W\|_\infty > \delta) &\leq \mathbf{p} \left[\exp \left\{ n \left\{ \frac{h^2}{2} (3 \log n)^2 n^\gamma \right\} - nh\delta \right\} \right. \\ &\quad \left. + \exp \left\{ n \left\{ \frac{h^2}{2} (3 \log n)^2 n^\gamma \right\} - nh\delta \right\} \right] + c_1 n^{-2} + c_2 n \kappa(n, \gamma) \\ &\leq 2\mathbf{p} \left[\exp \left\{ \frac{-n\delta^2}{18n^\gamma \log^2 n} \right\} \right] + c_1 n^{-2} + c_2 n \kappa(n, \gamma) \\ &\leq \exp\{-c_3 n\} + c_1 n^{-2} + c_2 n \kappa(n, \gamma), \end{aligned}$$

provided that $\mathbf{p} < \frac{1}{2} \exp \left(\frac{n^{1-\gamma} \delta^2}{36 \log^2 n} \right)$.

□

Theorem 2. Assume 1- 5. Then, there exists a non-negative decreasing sequence $\delta_n \rightarrow 0$, such that

$$\mathbb{P}_{\boldsymbol{\theta}} (\|\hat{\boldsymbol{\theta}}_s - \boldsymbol{\theta}_s\|_2 \leq \delta_n) \geq 1 - \exp\{-c_4 n^{1-2\gamma}\} - c_1 n^{-2} - c_2 n \kappa(n, \gamma), \quad \forall \boldsymbol{\theta} \in \boldsymbol{\Theta},$$

when $n \rightarrow \infty$.

Proof. For a fixed design \mathbb{X} , define $\mathbf{G} : \mathbb{R}^{p-1} \rightarrow \mathbb{R}$ as

$$G(\mathbf{u}, \mathbb{X}_s; \mathbb{X}_{V \setminus \{s\}}) = l(\boldsymbol{\theta}_s + \mathbf{u}, \mathbb{X}_s; \mathbb{X}_{V \setminus \{s\}}) - l(\boldsymbol{\theta}_s, \mathbb{X}_s; \mathbb{X}_{V \setminus \{s\}}).$$

Then, $\mathbf{G}(\mathbf{0}, \mathbb{X}_s; \mathbb{X}_{V \setminus \{s\}}) = 0$. Moreover, let $\hat{\mathbf{u}} = \hat{\boldsymbol{\theta}}_s - \boldsymbol{\theta}_s$, we have $\mathbf{G}(\hat{\mathbf{u}}, \mathbb{X}_s; \mathbb{X}_{V \setminus \{s\}}) \leq 0$.

Given a value $\epsilon > 0$, if $\mathbf{G}(\mathbf{u}, \mathbb{X}_s; \mathbb{X}_{V \setminus \{s\}}) > 0$, $\forall \mathbf{u} \in \mathbb{R}^{p-1}$ such that $\|\mathbf{u}\|_2 = \epsilon$, then $\|\hat{\mathbf{u}}\|_2 \leq \epsilon$, since $\mathbf{G}(\cdot, \mathbb{X}_s; \mathbb{X}_{V \setminus \{s\}})$ is a convex function. Therefore,

$$\mathbb{P}_{\boldsymbol{\theta}} \left(\|\hat{\boldsymbol{\theta}}_s - \boldsymbol{\theta}_s\|_2 \leq \epsilon \right) \geq \mathbb{P}_{\boldsymbol{\theta}} \left(G(\mathbf{u}, \mathbf{X}_s; \mathbf{X}_{V \setminus \{s\}}) > 0, \forall \mathbf{u} \in \mathbb{R}^{p-1} \text{ such that } \|\mathbf{u}\|_2 = \epsilon \right).$$

Using Taylor expansion of the node conditional log-likelihood at $\boldsymbol{\theta}_s$, we have

$$\begin{aligned} \mathbf{G}(\mathbf{u}) &= l(\boldsymbol{\theta}_s + \mathbf{u}, \mathbf{X}_s; \mathbf{X}_{V \setminus \{s\}}) - l(\boldsymbol{\theta}_s, \mathbf{X}_s; \mathbf{X}_{V \setminus \{s\}}) \\ &= \nabla l(\boldsymbol{\theta}_s, \mathbf{X}_s; \mathbf{X}_{V \setminus \{s\}}) \mathbf{u}^\top + \mathbf{u} [\nabla^2 l(\boldsymbol{\theta}_s + \mathbf{v}\mathbf{u}, \mathbf{X}_s; \mathbf{X}_{V \setminus \{s\}})] \mathbf{u}^\top, \end{aligned} \quad (\text{C11})$$

for some $\mathbf{v} \in [0, 1]$. Let

$$\begin{aligned} \mathbf{q} &= \Lambda_{\min}(\nabla^2 l(\boldsymbol{\theta}_s + \mathbf{v}\mathbf{u}, \mathbf{X}_s; \mathbf{X}_{V \setminus \{s\}})) \\ &\geq \min_{\mathbf{v} \in [0, 1]} \Lambda_{\min}(\nabla^2 l(\boldsymbol{\theta}_s + \mathbf{v}\mathbf{u}, \mathbf{X}_s; \mathbf{X}_{V \setminus \{s\}})) \\ &= \min_{\mathbf{v} \in [0, 1]} \Lambda_{\min} \left[\frac{1}{n} \sum_{i=1}^n D(\langle \boldsymbol{\theta}_s + \mathbf{v}\mathbf{u}, \mathbf{X}_{V \setminus \{s\}}^{(i)} \rangle) (\mathbf{X}_{V \setminus \{s\}}^{(i)})^\top \mathbf{X}_{V \setminus \{s\}}^{(i)} \right]. \end{aligned}$$

Using Taylor expansion for $D(\langle \boldsymbol{\theta}_s + \mathbf{v}\mathbf{u}, \mathbf{X}_{V \setminus \{s\}}^{(i)} \rangle)$ at $\langle \boldsymbol{\theta}_s, \mathbf{X}_{V \setminus \{s\}}^{(i)} \rangle$, we have

$$\begin{aligned} &\frac{1}{n} \sum_{i=1}^n D(\langle \boldsymbol{\theta}_s + \mathbf{v}\mathbf{u}, \mathbf{X}_{V \setminus \{s\}}^{(i)} \rangle) (\mathbf{X}_{V \setminus \{s\}}^{(i)})^\top \mathbf{X}_{V \setminus \{s\}}^{(i)} \\ &= \frac{1}{n} \sum_{i=1}^n D(\langle \boldsymbol{\theta}_s, \mathbf{X}_{V \setminus \{s\}}^{(i)} \rangle) (\mathbf{X}_{V \setminus \{s\}}^{(i)})^\top \mathbf{X}_{V \setminus \{s\}}^{(i)} + \\ &\quad \frac{1}{n} \sum_{i=1}^n D(\langle \boldsymbol{\theta}_s + \mathbf{v}'\mathbf{u}, \mathbf{X}_{V \setminus \{s\}}^{(i)} \rangle) [\mathbf{v}\mathbf{u} (\mathbf{X}_{V \setminus \{s\}}^{(i)})^\top] [(\mathbf{X}_{V \setminus \{s\}}^{(i)})^\top \mathbf{X}_{V \setminus \{s\}}^{(i)}], \end{aligned}$$

for some $\mathbf{v}' \in [0, 1]$. Hence,

$$\begin{aligned} \mathbf{q} &\geq \Lambda_{\min} \left[\frac{1}{n} \sum_{i=1}^n D(\langle \boldsymbol{\theta}_s, \mathbf{X}_{V \setminus \{s\}}^{(i)} \rangle) (\mathbf{X}_{V \setminus \{s\}}^{(i)})^\top \mathbf{X}_{V \setminus \{s\}}^{(i)} \right] \\ &\quad - \max_{\mathbf{v}' \in [0, 1]} \Lambda_{\max} \left[\frac{1}{n} \sum_{i=1}^n D(\langle \boldsymbol{\theta}_s + \mathbf{v}'\mathbf{u}, \mathbf{X}_{V \setminus \{s\}}^{(i)} \rangle) [\mathbf{u} (\mathbf{X}_{V \setminus \{s\}}^{(i)})^\top] [(\mathbf{X}_{V \setminus \{s\}}^{(i)})^\top \mathbf{X}_{V \setminus \{s\}}^{(i)}] \right]. \end{aligned}$$

Define a new event

$$\zeta_3 = \{ \langle \boldsymbol{\theta}_s + \mathbf{v}'\mathbf{u}, \mathbf{X}_{V \setminus \{s\}}^{(i)} \rangle \leq \gamma \log n \}.$$

Similarly to the event ζ_2 , we have $\mathbb{P}_{\boldsymbol{\theta}}(\zeta_3) \leq c_2 n \kappa(n, \gamma) + c_1 n^{-2}$, provided that $\epsilon \leq \frac{1}{3p \log n}$. As consequence, $|D(\langle \boldsymbol{\theta}_s + \mathbf{v}'\mathbf{u}, \mathbf{X}_{V \setminus \{s\}}^{(i)} \rangle)| \leq n^\gamma$,

with probability at least $1 - c_2 n \kappa(n, \gamma) - c_1 n^{-2}$. Fixed $\delta = \frac{\lambda_{\min}}{8}$ in Lemma C.1, and conditioned on ζ_1, ζ_3 we have

$$\begin{aligned} \mathbf{q} &\geq \lambda_{\min} - \delta - \max_{\mathbf{v}' \in [0, 1]} \Lambda_{\max} \left[\frac{1}{n} \sum_{i=1}^n D(\langle \boldsymbol{\theta}_s + \mathbf{v}'\mathbf{u}, \mathbf{X}_{V \setminus \{s\}}^{(i)} \rangle) [\mathbf{u} (\mathbf{X}_{V \setminus \{s\}}^{(i)})^\top] [(\mathbf{X}_{V \setminus \{s\}}^{(i)})^\top \mathbf{X}_{V \setminus \{s\}}^{(i)}] \right] \\ &\geq \lambda_{\min} - \delta - \max_{\mathbf{v}' \in [0, 1]} |D(\langle \boldsymbol{\theta}_s + \mathbf{v}'\mathbf{u}, \mathbf{X}_{V \setminus \{s\}}^{(i)} \rangle)| |\mathbf{u} (\mathbf{X}_{V \setminus \{s\}}^{(i)})^\top| \Lambda_{\max} \left[\frac{1}{n} \sum_{i=1}^n (\mathbf{X}_{V \setminus \{s\}}^{(i)})^\top \mathbf{X}_{V \setminus \{s\}}^{(i)} \right] \\ &\geq \lambda_{\min} - 2\delta - n^\gamma 3 \log n \sqrt{p} \|\mathbf{u}\|_2 \lambda_{\max} \\ &= \lambda_{\min} - 2\delta - 3\sqrt{p} \epsilon \lambda_{\max} n^\gamma \log n \\ &\geq \frac{\lambda_{\min}}{2}, \quad \text{provided that } \epsilon < \frac{\lambda_{\min}}{12\sqrt{p} \lambda_{\max} n^\gamma \log n}, \end{aligned}$$

with probability at least $1 - \exp\{-c_4 n\} - c_2 n \kappa(n, \gamma) - c_1 n^{-2}$. Let $\delta = \frac{\lambda_{\min}}{2} \epsilon$ in Proposition C.2, we have

$$\nabla_t l(\boldsymbol{\theta}_s, \mathbf{X}_s; \mathbf{X}_{V \setminus \{s\}}) > -\frac{\lambda_{\min}}{2} \epsilon,$$

with probability at least $1 - \exp\{-c_3 n\} - c_2 n \kappa(n, \gamma) - c_1 n^{-2}$, provided that $p < \frac{1}{2} \exp\left(\frac{n^{1-\gamma} \lambda_{\min}^2 \epsilon^2}{144 \log^2 n}\right)$. Combining with the inequality of q , we have

$$\begin{aligned} \mathbf{G}(\mathbf{u}) &= \nabla l(\boldsymbol{\theta}_s, \mathbf{X}_s; \mathbf{X}_{V \setminus \{s\}}) \mathbf{u}^\top + \mathbf{u} [\nabla^2 l(\boldsymbol{\theta}_s + \mathbf{v} \mathbf{u}_s, \mathbf{X}_s; \mathbf{X}_{V \setminus \{s\}})] \mathbf{u}^\top \\ &> -\frac{\lambda_{\min}}{2} \epsilon^2 + \frac{\lambda_{\min}}{2} \epsilon^2 = 0 \end{aligned} \quad (\text{C12})$$

provided that $\epsilon < \frac{\lambda_{\min}}{12\sqrt{p}\lambda_{\max}n^\gamma \log n}$, and $p < \frac{1}{2} \exp\left(\frac{n^{1-\gamma} \lambda_{\min}^2 \epsilon^2}{144 \log^2 n}\right)$. It means that $\|\hat{\mathbf{u}}\|_2 < \epsilon$. When $n \rightarrow \infty$ we can choose a non-negative decreasing sequence δ_n such that $\delta_n < \frac{\lambda_{\min}}{12\sqrt{p}\lambda_{\max}n^\gamma \log n}$, then

$$\begin{aligned} \mathbb{P}_{\boldsymbol{\theta}}(\|\hat{\boldsymbol{\theta}}_{V \setminus \{s\}} - \boldsymbol{\theta}_{V \setminus \{s\}}\|_2 \leq \delta_n) &\geq 1 - \exp\{-c_4 n\} - \exp\{-c_3 n\} - c_2 n \kappa(n, \gamma) - c_1 n^{-2} \\ &= 1 - \exp\{-cn\} - c_2 n \kappa(n, \gamma) - c_1 n^{-2} \end{aligned}$$

when $n \rightarrow \infty$. □

Results for $\mathbf{K} \subset \mathbf{V}$ are derived as following.

Proposition C.3. Assume 1- 5 and let $\mathbf{K} \subset \mathbf{V}$. Then, for all $s \in \mathbf{K}$ and any $\delta > 0$

$$\mathbb{P}_{\boldsymbol{\theta}}(\|\nabla l(\boldsymbol{\theta}_{s|\mathbf{K}}, \mathbf{X}_{\{s\}}; \mathbf{X}_{\mathbf{K} \setminus \{s\}})\|_\infty \geq \delta) \leq \exp\{-c_3 n\} + c_2 \kappa(n, \gamma) + c_1 n^{-2},$$

$\forall \boldsymbol{\theta}_{s|\mathbf{K}} \in \boldsymbol{\Theta}$, when $n \rightarrow \infty$.

Proof. The proof of Proposition C.3 follows the lines of Proposition C.2. We note that the set of explanatory variables $\mathbf{X}_{\mathbf{K} \setminus \{s\}}$ in the generalized linear model \mathbf{X}_s given $\mathbf{X}_{\mathbf{K} \setminus \{s\}}$ does not include variables \mathbf{X}_t , with $t \in \mathbf{V} \setminus \mathbf{K}$. Suppose we zero-pad the true parameter $\boldsymbol{\theta}_{s|\mathbf{K}} \in \mathbb{R}^{|\mathbf{K}|-1}$ to include zero weights over $\mathbf{V} \setminus \mathbf{K}$, then the resulting parameter would lie in \mathbb{R}^{p-1} . □

Note C.4. When the maximum number of neighbours that one node is allowed to have is fixed, a control is operated on the cardinality of the set \mathbf{K} , $|\mathbf{K}| \leq m + 1$. In this case, parameters $\boldsymbol{\theta}_{st|\mathbf{K}}$ are estimated from models that are restricted on subsets of variables with their cardinalities less than or equal to $m + 1$. Therefore, p in Proposition C.2 is replaced by $m + 1$. In detail, for all $s \in \mathbf{K}$ and any $\delta > 0$

$$\mathbb{P}_{\boldsymbol{\theta}}(\|\nabla l(\boldsymbol{\theta}_{s|\mathbf{K}}, \mathbf{X}_{\{s\}}; \mathbf{X}_{\mathbf{K} \setminus \{s\}})\|_\infty \geq \delta) \leq \exp\{-c_3 n\} + c_2 \kappa(n, \gamma) + c_1 n^{-2},$$

$\forall \boldsymbol{\theta}_{s|\mathbf{K}} \in \boldsymbol{\Theta}$, provided that $m < \frac{1}{2} \exp\left\{\frac{n^{1-\gamma} \delta^2}{36 \log^2 n}\right\}$.

Theorem 3. Assume 1- 5 and let $\mathbf{K} \subset \mathbf{V}$. Then, there exists a non-negative decreasing sequence $\delta_n \rightarrow 0$, such that

$$\mathbb{P}_{\boldsymbol{\theta}}(\|\hat{\boldsymbol{\theta}}_{s|\mathbf{K}} - \boldsymbol{\theta}_{s|\mathbf{K}}\|_2 \leq \delta_n) \geq 1 - \exp\{-cn\} - c_2 n \kappa(n, \gamma) - c_1 n^{-2}, \quad \forall s \in \mathbf{K}, \boldsymbol{\theta} \in \boldsymbol{\Theta},$$

when $n \rightarrow \infty$.

Proof. Theorem 3 is proved by following the lines of Theorem 3. The difference lies in the set of explanatory variables $\mathbf{X}_{\mathbf{K} \setminus \{s\}}$. As consequence, it is necessary to control the spectral norm of the submatrices, $\mathbf{Q}_{s|\mathbf{K}}(\boldsymbol{\theta}_{s|\mathbf{K}}) = \frac{1}{n} \sum_{i=1}^n \mathbf{D}(\langle \boldsymbol{\theta}_{s|\mathbf{K}}, \mathbf{X}_{\mathbf{K} \setminus \{s\}}^{(i)} \rangle) (\mathbf{X}_{\mathbf{K} \setminus \{s\}}^{(i)})^\top \mathbf{X}_{\mathbf{K} \setminus \{s\}}^{(i)}$ and $(\mathbf{X}_{\mathbf{K} \setminus \{s\}}^{(i)})^\top \mathbf{X}_{\mathbf{K} \setminus \{s\}}^{(i)}$. Here, we employ well-known results on eigenvalue inequalities for a matrix and its submatrix (see, for example, Johnson & Robinson 1981), that is,

$$\Lambda_{\min} [\mathbf{Q}_{s|\mathbf{K}}(\boldsymbol{\theta}_{s|\mathbf{K}})] \geq \Lambda_{\min}(\mathbf{Q}_s(\boldsymbol{\theta}_s)) \geq \lambda_{\min} - \delta,$$

and,

$$\Lambda_{\max} \left[\frac{1}{n} \sum_{i=1}^n (\mathbf{X}_{\mathbf{K} \setminus \{s\}}^{(i)})^\top \mathbf{X}_{\mathbf{K} \setminus \{s\}}^{(i)} \right] \leq \Lambda_{\max} \left[\frac{1}{n} \sum_{i=1}^n (\mathbf{X}_{\mathbf{V} \setminus \{s\}}^{(i)})^\top \mathbf{X}_{\mathbf{V} \setminus \{s\}}^{(i)} \right] \leq \lambda_{\max} + \delta.$$

Then, by performing the same analysis as in the proof of Theorem 2 and using the result of Proposition C.3, we get the result. □

Note C.5. In the proof of Theorem 3, we only require the uniform convergence of a submatrix (restricted on \mathbf{K}), $\mathbf{Q}_{s|\mathbf{K}}(\boldsymbol{\theta}_{s|\mathbf{K}})$, of the sample Fisher information matrix $\mathbf{Q}_s(\boldsymbol{\theta}_s)$. Therefore, when the maximum neighbourhood size is known, $|\mathbf{K}| \leq m + 1$, we have convergence provided that $n > \mathcal{O}_p(\log m)$. In detail, let $\mathbf{l}_{s|\mathbf{K}}(\boldsymbol{\theta}_{s|\mathbf{K}})$ be the submatrix of $\mathbf{l}_s(\boldsymbol{\theta}_s)$ indexed in \mathbf{K} , Equation (C6) becomes

$$\begin{aligned} \mathbb{P}_{\boldsymbol{\theta}}(\|\mathbf{l}_{s|\mathbf{K}}(\boldsymbol{\theta}_{s|\mathbf{K}}) - \mathbf{Q}_{s|\mathbf{K}}(\boldsymbol{\theta}_{s|\mathbf{K}})\|_2 \geq \delta) &\leq \mathbb{P}_{\boldsymbol{\theta}}\left(\left(\sum_{j,k \in \mathbf{K} \setminus \{s\}} (Z_{jk}^n)^2\right)^{1/2} \geq \delta\right) \\ &\leq 2m^2 \exp\left\{-\frac{\delta^2 n}{36p^2 n^{2\gamma} \log^4 n}\right\} + c_2 \kappa(n, \gamma) + c_1 n^{-2} \\ &\leq \exp\{-c_4 n\} + c_2 \kappa(n, \gamma) + c_1 n^{-2}, \end{aligned}$$

provided that $n > \mathcal{O}_p(\log m)$.

D ADDITIONAL RESULTS IN EMPIRICAL STUDY

D.1 Tables

Table D.1, and Table D.2 report TP, FP, FN, P, R and F_1 for each of methods considered in Section 5 of the main paper and for the three types of networks. Two different graph dimensions, i.e., $p = 10, 100$, and three graph structures (see Figure 1 and Figure 2 in the main paper) are considered.

TABLE D.1 Simulation results from 50 replicates of the DAGs shown in Figure 1 in of the main paper for $p = 10$ variables with Poisson node conditional distribution. Monte Carlo means (standard deviations) are shown for TP, FP, FN, P, R, and F_1 . The levels of significance of tests $\alpha = 2(1 - \Phi(n^{0.15}))$.

Graph	n	Algorithm	TP	FP	FN	P	R	F_1	time
Scale-free	100	PKBIC	6.300(1.129)	1.140(1.069)	2.700(1.129)	0.857(0.123)	0.700(0.125)	0.764(0.106)	0.147
		Or-PPGM	5.520(1.147)	1.060(1.219)	3.480(1.147)	0.859(0.151)	0.613(0.127)	0.706(0.114)	0.880
		Or-LPGM	6.260(1.084)	1.600(1.107)	2.740(1.084)	0.807(0.103)	0.696(0.120)	0.740(0.093)	0.063
		PDN	7.680(0.741)	27.740(4.716)	1.320(0.741)	0.221(0.037)	0.853(0.082)	0.350(0.051)	0.103
		ODS	2.500(1.052)	1.292(0.967)	6.500(1.052)	0.670(0.209)	0.278(0.117)	0.384(0.145)	3.492
		PC	3.440(1.128)	2.780(1.389)	5.560(1.128)	0.564(0.169)	0.382(0.125)	0.450(0.135)	0.007
		MMHC	2.061(0.944)	3.551(1.138)	6.939(0.944)	0.367(0.144)	0.229(0.105)	0.279(0.116)	0.005
	200	PKBIC	7.840(0.912)	0.660(1.062)	1.160(0.912)	0.932(0.100)	0.871(0.101)	0.896(0.083)	0.160
		Or-PPGM	7.300(1.313)	0.500(0.909)	1.700(1.313)	0.947(0.088)	0.811(0.146)	0.864(0.097)	0.501
		Or-LPGM	7.580(0.906)	0.660(0.982)	1.420(0.906)	0.930(0.096)	0.842(0.101)	0.879(0.077)	0.064
		PDN	8.380(0.697)	21.160(4.157)	0.620(0.697)	0.289(0.051)	0.931(0.077)	0.440(0.063)	0.106
		ODS	3.740(0.922)	1.880(1.206)	5.260(0.922)	0.683(0.181)	0.416(0.102)	0.511(0.118)	3.841
		PC	5.020(0.892)	2.400(1.010)	3.980(0.892)	0.681(0.103)	0.558(0.099)	0.610(0.093)	0.007
		MMHC	3.160(1.113)	4.460(1.388)	5.840(1.113)	0.417(0.137)	0.351(0.124)	0.379(0.126)	0.007
	500	PKBIC	8.780(0.418)	0.540(0.706)	0.220(0.418)	0.947(0.067)	0.976(0.046)	0.959(0.044)	0.204
		Or-PPGM	8.380(0.805)	0.360(0.598)	0.620(0.805)	0.962(0.064)	0.931(0.089)	0.944(0.062)	0.549
		Or-LPGM	8.480(0.544)	0.380(0.567)	0.520(0.544)	0.961(0.058)	0.942(0.060)	0.950(0.043)	0.033
		PDN	8.540(0.579)	14.280(1.938)	0.460(0.579)	0.376(0.032)	0.949(0.064)	0.538(0.036)	0.116
		ODS	5.100(1.035)	2.360(1.258)	3.900(1.035)	0.692(0.142)	0.567(0.115)	0.620(0.118)	4.717
		PC	5.820(0.850)	2.500(0.863)	3.180(0.850)	0.701(0.096)	0.647(0.094)	0.672(0.092)	0.008
		MMHC	4.040(1.340)	4.820(1.224)	4.960(1.340)	0.453(0.137)	0.449(0.149)	0.450(0.142)	0.008
	1000	PKBIC	8.940(0.240)	0.360(0.598)	0.060(0.240)	0.965(0.057)	0.993(0.027)	0.978(0.035)	0.271
		Or-PPGM	8.820(0.482)	0.120(0.328)	0.180(0.482)	0.988(0.033)	0.980(0.054)	0.983(0.032)	0.956
		Or-LPGM	8.840(0.370)	0.260(0.527)	0.160(0.370)	0.974(0.052)	0.982(0.041)	0.977(0.038)	0.065
		PDN	8.660(0.479)	10.480(1.359)	0.340(0.479)	0.454(0.034)	0.962(0.053)	0.616(0.036)	0.137
		ODS	5.820(1.024)	2.840(1.283)	3.180(1.024)	0.679(0.126)	0.647(0.114)	0.660(0.112)	5.690
		PC	6.420(0.906)	2.360(0.776)	2.580(0.906)	0.730(0.088)	0.713(0.101)	0.721(0.093)	0.008
		MMHC	4.960(1.087)	4.420(0.971)	4.040(1.087)	0.527(0.104)	0.551(0.121)	0.538(0.110)	0.010
100	PKBIC	5.480(1.035)	1.500(1.111)	2.520(1.035)	0.800(0.134)	0.685(0.129)	0.730(0.104)	0.149	
	Or-PPGM	4.600(1.678)	1.580(1.230)	3.400(1.678)	0.755(0.178)	0.575(0.210)	0.633(0.183)	0.914	
	Or-LPGM	5.640(1.025)	1.920(1.469)	2.360(1.025)	0.768(0.144)	0.705(0.128)	0.725(0.104)	0.064	
	PDN	5.180(1.101)	33.300(4.022)	2.820(1.101)	0.135(0.029)	0.647(0.138)	0.224(0.047)	0.104	
	ODS	1.449(0.614)	0.347(0.597)	6.551(0.614)	0.881(0.201)	0.181(0.077)	0.289(0.097)	3.551	
	PC	2.920(1.104)	2.200(1.294)	5.080(1.104)	0.579(0.201)	0.365(0.138)	0.443(0.158)	0.007	

TABLE D.1 – continued from previous page

Graph	n	Algorithm	TP	FP	FN	P	R	F ₁	time	
Hub	200	MMHC	1.122(0.400)	3.732(1.225)	6.878(0.400)	0.243(0.090)	0.140(0.050)	0.175(0.058)	0.005	
		PKBIC	6.300(0.814)	0.680(0.819)	1.700(0.814)	0.911(0.103)	0.787(0.102)	0.840(0.083)	0.166	
		Or-PPGM	5.580(1.444)	0.680(0.741)	2.420(1.444)	0.901(0.108)	0.698(0.181)	0.771(0.142)	0.510	
		Or-LPGM	6.280(0.858)	0.980(0.937)	1.720(0.858)	0.877(0.111)	0.785(0.107)	0.822(0.082)	0.065	
		PDN	5.660(1.171)	31.240(3.679)	2.340(1.171)	0.154(0.030)	0.708(0.146)	0.252(0.049)	0.107	
		ODS	2.560(0.951)	0.700(0.789)	5.440(0.951)	0.810(0.193)	0.320(0.119)	0.446(0.136)	4.002	
		PC	4.640(1.102)	1.400(0.808)	3.360(1.102)	0.766(0.138)	0.580(0.138)	0.656(0.133)	0.008	
	MMHC	1.122(0.726)	5.082(1.272)	6.878(0.726)	0.185(0.105)	0.140(0.091)	0.158(0.096)	0.007		
	500	PKBIC	7.460(0.503)	0.560(0.705)	0.540(0.503)	0.935(0.077)	0.932(0.063)	0.932(0.057)	0.217	
		Or-PPGM	7.240(0.744)	0.480(0.646)	0.760(0.744)	0.942(0.076)	0.905(0.093)	0.920(0.072)	0.549	
		Or-LPGM	7.380(0.635)	0.360(0.663)	0.620(0.635)	0.959(0.072)	0.922(0.079)	0.937(0.059)	0.037	
		PDN	5.560(1.198)	22.960(4.755)	2.440(1.198)	0.200(0.045)	0.695(0.150)	0.305(0.053)	0.118	
		ODS	4.680(1.096)	1.280(1.089)	3.320(1.096)	0.795(0.164)	0.585(0.137)	0.668(0.136)	5.239	
		PC	6.300(1.129)	1.000(1.294)	1.700(1.129)	0.869(0.162)	0.787(0.141)	0.825(0.147)	0.009	
		MMHC	1.188(0.641)	6.354(1.041)	6.812(0.641)	0.157(0.072)	0.148(0.080)	0.152(0.075)	0.008	
	1000	PKBIC	7.820(0.388)	0.340(0.519)	0.180(0.388)	0.962(0.058)	0.978(0.049)	0.968(0.041)	0.297	
		Or-PPGM	7.700(0.463)	0.140(0.351)	0.300(0.463)	0.984(0.040)	0.963(0.058)	0.972(0.037)	0.999	
		Or-LPGM	7.780(0.418)	0.160(0.370)	0.220(0.418)	0.982(0.043)	0.973(0.052)	0.976(0.036)	0.073	
		PDN	5.800(1.370)	18.880(3.910)	2.200(1.370)	0.238(0.044)	0.725(0.171)	0.353(0.065)	0.138	
		ODS.3	5.660(0.872)	1.940(1.346)	2.340(0.872)	0.762(0.140)	0.708(0.109)	0.728(0.104)	7.062	
		PC	7.120(1.003)	0.540(1.110)	0.880(1.003)	0.933(0.131)	0.890(0.125)	0.910(0.125)	0.009	
		MMHC	1.468(1.080)	6.660(1.069)	6.532(1.080)	0.176(0.113)	0.184(0.135)	0.179(0.123)	0.009	
	Random	100	PKBIC	3.620(1.210)	1.540(1.014)	4.380(1.210)	0.717(0.158)	0.452(0.151)	0.539(0.146)	0.134
			Or-PPGM	3.600(1.355)	1.500(0.974)	4.400(1.355)	0.709(0.170)	0.450(0.169)	0.536(0.165)	0.864
			Or-LPGM	3.700(1.344)	1.700(1.182)	4.300(1.344)	0.699(0.183)	0.462(0.168)	0.540(0.165)	0.063
			PDN	5.700(1.015)	36.800(4.020)	2.300(1.015)	0.135(0.024)	0.713(0.127)	0.226(0.040)	0.104
			ODS	1.250(0.568)	0.438(0.619)	6.750(0.568)	0.816(0.242)	0.156(0.071)	0.253(0.089)	3.458
PC			1.590(0.751)	2.897(0.995)	6.410(0.751)	0.355(0.129)	0.199(0.094)	0.251(0.106)	0.006	
MMHC			1.894(0.699)	2.043(1.122)	6.106(0.699)	0.516(0.208)	0.237(0.087)	0.315(0.105)	0.005	
200		PKBIC	4.740(1.226)	0.740(0.944)	3.260(1.226)	0.879(0.141)	0.593(0.153)	0.696(0.132)	0.140	
		Or-PPGM	4.680(1.253)	0.860(0.990)	3.320(1.253)	0.864(0.150)	0.585(0.157)	0.683(0.133)	0.457	
		Or-LPGM	4.660(1.206)	0.960(1.195)	3.340(1.206)	0.853(0.166)	0.583(0.151)	0.679(0.134)	0.065	
		PDN	6.420(1.012)	34.060(4.688)	1.580(1.012)	0.160(0.029)	0.802(0.126)	0.267(0.045)	0.108	
		ODS	1.568(0.695)	1.114(0.993)	6.432(0.695)	0.639(0.280)	0.196(0.087)	0.293(0.120)	3.919	
		PC	2.356(1.282)	2.222(0.974)	5.644(1.282)	0.499(0.193)	0.294(0.160)	0.364(0.174)	0.006	
		MMHC	2.680(1.115)	2.060(1.185)	5.320(1.115)	0.571(0.191)	0.335(0.139)	0.416(0.155)	0.006	
500		PKBIC	6.540(0.838)	0.460(0.579)	1.460(0.838)	0.938(0.077)	0.818(0.105)	0.870(0.077)	0.163	
		Or-PPGM	6.400(0.881)	0.460(0.613)	1.600(0.881)	0.938(0.081)	0.800(0.110)	0.859(0.080)	0.543	
		Or-LPGM	6.300(0.789)	0.420(0.609)	1.700(0.789)	0.944(0.079)	0.787(0.099)	0.854(0.069)	0.032	
		PDN	7.100(0.735)	29.300(3.066)	0.900(0.735)	0.196(0.025)	0.887(0.092)	0.321(0.039)	0.119	
		ODS	3.260(1.275)	1.800(1.262)	4.740(1.275)	0.655(0.209)	0.408(0.159)	0.493(0.168)	4.924	
		PC	4.204(1.399)	2.020(0.989)	3.796(1.399)	0.666(0.174)	0.526(0.175)	0.585(0.173)	0.007	
		MMHC	4.700(1.055)	2.000(1.178)	3.300(1.055)	0.710(0.140)	0.588(0.132)	0.638(0.126)	0.007	
1000		PKBIC	7.520(0.580)	0.360(0.598)	0.480(0.580)	0.960(0.065)	0.940(0.072)	0.947(0.046)	0.216	
		Or-PPGM	7.200(0.782)	0.280(0.454)	0.800(0.782)	0.965(0.057)	0.900(0.098)	0.928(0.065)	0.924	
		Or-LPGM	7.020(0.820)	0.120(0.385)	0.980(0.820)	0.985(0.048)	0.877(0.103)	0.925(0.064)	0.057	
		PDN	7.460(0.676)	24.420(2.417)	0.540(0.676)	0.235(0.024)	0.932(0.085)	0.375(0.035)	0.139	
		ODS	4.160(1.315)	2.800(1.414)	3.840(1.315)	0.602(0.186)	0.520(0.164)	0.556(0.169)	6.144	
		PC	5.160(1.095)	1.640(0.631)	2.840(1.095)	0.753(0.111)	0.645(0.137)	0.693(0.124)	0.008	
	MMHC	5.420(0.992)	2.040(1.029)	2.580(0.992)	0.729(0.129)	0.677(0.124)	0.701(0.121)	0.009		

TABLE D.2 Simulation results from 50 replicates of the DAGs shown in Figure 2 in of the main paper for $p = 100$ variables with Poisson node conditional distribution. Monte Carlo means (standard deviations) are shown for TP, FP, FN, P, R, and F₁. The levels of significance of tests $\alpha = 2(1 - \Phi(n^{0.2}))$ for $n = 500, 1000, 2000$, and $\alpha = 2(1 - \Phi(n^{0.225}))$ for $n = 200$.

Graph	n	Algorithm	TP	FP	FN	P	R	F ₁	time
	200	PKBIC	72.800(3.597)	74.360(6.608)	26.200(3.597)	0.495(0.029)	0.735(0.036)	0.592(0.030)	2.966

TABLE D.2 – continued from previous page

Graph	n	Algorithm	TP	FP	FN	P	R	F ₁	time	
Scale-free	500	Or-PPGM	53.080(2.947)	5.880(2.336)	45.920(2.947)	0.901(0.036)	0.536(0.030)	0.672(0.027)	3.062	
		Or-LPGM	42.740(3.096)	7.040(9.689)	56.260(3.096)	0.875(0.085)	0.432(0.031)	0.575(0.035)	0.136	
		PDN	49.220(15.953)	277.140(163.948)	49.780(15.953)	0.241(0.198)	0.497(0.161)	0.244(0.079)	3.876	
		ODS	33.800(5.051)	106.700(31.538)	65.200(5.051)	0.250(0.046)	0.341(0.051)	0.284(0.033)	108.155	
		PC	24.280(2.458)	20.980(3.191)	74.720(2.458)	0.538(0.054)	0.245(0.025)	0.337(0.032)	0.097	
		MMHC	35.400(4.041)	95.500(6.935)	63.600(4.041)	0.271(0.032)	0.358(0.041)	0.308(0.035)	0.367	
		PKBIC	86.980(1.890)	45.420(6.970)	12.020(1.890)	0.659(0.037)	0.879(0.019)	0.752(0.027)	4.237	
		Or-PPGM	74.900(3.604)	3.540(1.705)	24.100(3.604)	0.955(0.021)	0.757(0.036)	0.844(0.025)	3.944	
		Or-LPGM	74.560(2.822)	2.200(1.604)	24.440(2.822)	0.972(0.019)	0.753(0.029)	0.848(0.019)	0.236	
		PDN	48.520(23.784)	111.880(87.858)	50.480(23.784)	0.417(0.202)	0.490(0.240)	0.351(0.134)	4.831	
		ODS	45.740(5.938)	94.840(32.950)	53.260(5.938)	0.340(0.062)	0.462(0.060)	0.385(0.039)	195.076	
		PC	39.940(3.158)	28.800(3.090)	59.060(3.158)	0.581(0.040)	0.403(0.032)	0.476(0.034)	0.123	
	MMHC	55.220(5.152)	86.880(7.634)	43.780(5.152)	0.389(0.037)	0.558(0.052)	0.458(0.042)	0.530		
	1000	PKBIC	92.265(0.995)	32.755(5.329)	6.735(0.995)	0.739(0.032)	0.932(0.010)	0.824(0.020)	6.558	
		Or-PPGM	83.286(3.234)	1.184(1.034)	15.714(3.234)	0.986(0.012)	0.841(0.033)	0.908(0.020)	5.066	
		Or-LPGM	85.600(2.268)	0.240(0.476)	13.400(2.268)	0.997(0.005)	0.865(0.023)	0.926(0.013)	0.398	
		PDN	45.980(26.072)	63.160(52.492)	53.020(26.072)	0.538(0.197)	0.464(0.263)	0.399(0.162)	6.473	
		ODS	51.580(12.993)	84.300(31.210)	47.420(12.993)	0.404(0.090)	0.521(0.131)	0.431(0.083)	307.384	
		PC	46.880(2.862)	32.740(2.841)	52.120(2.862)	0.589(0.031)	0.474(0.029)	0.525(0.028)	0.152	
		MMHC	66.760(4.770)	73.200(7.157)	32.240(4.770)	0.478(0.040)	0.674(0.048)	0.559(0.043)	0.825	
		2000	PKBIC	93.840(0.370)	22.080(4.575)	5.160(0.370)	0.811(0.033)	0.948(0.004)	0.874(0.019)	11.046
			Or-PPGM	89.120(2.086)	1.500(0.735)	9.880(2.086)	0.984(0.008)	0.900(0.021)	0.940(0.012)	9.026
			Or-LPGM	93.760(1.697)	0.020(0.141)	5.240(1.697)	1.000(0.002)	0.947(0.017)	0.973(0.009)	0.754
			PDN	34.540(23.652)	33.940(28.183)	64.460(23.652)	0.594(0.160)	0.349(0.239)	0.360(0.189)	10.075
ODS			61.840(13.864)	95.280(32.128)	37.160(13.864)	0.403(0.074)	0.625(0.140)	0.477(0.088)	516.160	
PC	54.200(2.563)		35.640(2.855)	44.800(2.563)	0.603(0.029)	0.547(0.026)	0.574(0.027)	0.195		
MMHC	73.900(4.082)	60.580(7.535)	25.100(4.082)	0.551(0.042)	0.746(0.041)	0.634(0.041)	1.396			
Hub	200	PKBIC	44.540(3.759)	88.800(7.635)	50.460(3.759)	0.335(0.028)	0.469(0.040)	0.390(0.030)	2.848	
		Or-PPGM	19.000(3.608)	5.180(2.396)	76.000(3.608)	0.787(0.096)	0.200(0.038)	0.318(0.052)	2.658	
		Or-LPGM	11.080(2.448)	5.920(2.687)	83.920(2.448)	0.659(0.116)	0.117(0.026)	0.197(0.040)	0.146	
		PDN	40.540(4.807)	723.700(69.012)	54.460(4.807)	0.054(0.009)	0.427(0.051)	0.095(0.013)	3.896	
		ODS	8.540(3.981)	60.700(30.999)	86.460(3.981)	0.138(0.073)	0.090(0.042)	0.104(0.046)	86.450	
		PC	2.000(1.155)	13.326(2.504)	93.000(1.155)	0.131(0.068)	0.021(0.012)	0.036(0.020)	0.091	
		MMHC	18.720(3.226)	99.040(7.546)	76.280(3.226)	0.159(0.029)	0.197(0.034)	0.176(0.031)	0.389	
		500	PKBIC	66.920(2.884)	55.360(5.713)	28.080(2.884)	0.548(0.025)	0.704(0.030)	0.616(0.021)	3.967
	Or-PPGM		49.120(4.094)	3.040(1.340)	45.880(4.094)	0.942(0.024)	0.517(0.043)	0.667(0.037)	3.103	
	Or-LPGM		37.500(4.735)	2.700(1.632)	57.500(4.735)	0.934(0.039)	0.395(0.050)	0.553(0.051)	0.238	
	PDN		60.980(3.396)	653.320(42.419)	34.020(3.396)	0.086(0.005)	0.642(0.036)	0.151(0.008)	4.852	
	ODS		18.340(8.178)	72.520(28.367)	76.660(8.178)	0.211(0.101)	0.193(0.086)	0.194(0.079)	145.684	
	PC		5.000(1.539)	24.060(2.189)	90.000(1.539)	0.171(0.049)	0.053(0.016)	0.080(0.024)	0.350	
	MMHC		37.260(4.580)	84.720(10.236)	57.740(4.580)	0.307(0.046)	0.392(0.048)	0.344(0.046)	9.120	
	1000		PKBIC	75.260(1.291)	38.440(5.588)	19.740(1.291)	0.663(0.034)	0.792(0.014)	0.722(0.023)	5.987
		Or-PPGM	67.760(3.503)	0.320(0.513)	27.240(3.503)	0.995(0.007)	0.713(0.037)	0.830(0.026)	4.147	
		Or-LPGM	57.420(3.844)	0.240(0.431)	37.580(3.844)	0.996(0.008)	0.604(0.040)	0.751(0.032)	0.402	
		PDN	69.200(2.441)	546.600(20.849)	25.800(2.441)	0.112(0.005)	0.728(0.026)	0.195(0.008)	6.503	
		ODS	26.280(9.311)	92.760(12.697)	68.720(9.311)	0.221(0.076)	0.277(0.098)	0.245(0.085)	232.417	
		PC	7.760(1.533)	34.260(2.221)	87.240(1.533)	0.185(0.036)	0.082(0.016)	0.113(0.022)	4.832	
		MMHC	53.740(4.931)	71.900(9.429)	41.260(4.931)	0.429(0.047)	0.566(0.052)	0.488(0.047)	358.392	
		2000	PKBIC	77.520(0.544)	26.240(4.897)	17.480(0.544)	0.749(0.034)	0.816(0.006)	0.780(0.019)	9.937
	Or-PPGM		80.800(2.755)	0.040(0.198)	14.200(2.755)	0.999(0.002)	0.851(0.029)	0.919(0.017)	9.954	
	Or-LPGM		76.020(2.317)	0.000(0.000)	18.980(2.317)	1.000(0.000)	0.800(0.024)	0.889(0.015)	0.754	
PDN	71.100(2.188)		421.220(30.434)	23.900(2.188)	0.145(0.009)	0.748(0.023)	0.243(0.013)	10.005		
ODS	36.020(11.302)		82.320(12.173)	58.980(11.302)	0.304(0.093)	0.379(0.119)	0.337(0.104)	397.424		
PC	12.460(2.111)		46.800(2.304)	82.540(2.111)	0.210(0.029)	0.131(0.022)	0.161(0.025)	86.424		
MMHC	66.000(7.323)		57.440(10.459)	29.000(7.323)	0.537(0.069)	0.695(0.077)	0.605(0.072)	3351.923		
200	PKBIC		63.320(3.554)	80.180(6.998)	45.680(3.554)	0.442(0.028)	0.581(0.033)	0.502(0.028)	3.024	
	Or-PPGM	33.840(4.063)	4.900(2.063)	75.160(4.063)	0.875(0.046)	0.310(0.037)	0.457(0.042)	2.760		
	Or-LPGM	24.500(2.589)	6.060(2.385)	84.500(2.589)	0.805(0.064)	0.225(0.024)	0.351(0.031)	0.140		
	PDN	61.980(4.354)	641.620(23.913)	47.020(4.354)	0.088(0.007)	0.569(0.040)	0.153(0.012)	3.866		
	ODS	27.900(6.112)	108.440(32.255)	81.100(6.112)	0.215(0.054)	0.256(0.056)	0.227(0.035)	91.828		
	PC	15.180(3.330)	15.040(3.201)	93.820(3.330)	0.502(0.090)	0.139(0.031)	0.217(0.045)	0.089		
	MMHC	28.460(3.877)	102.080(7.331)	80.540(3.877)	0.218(0.029)	0.261(0.036)	0.238(0.031)	0.357		

TABLE D.2 – continued from previous page

Graph	n	Algorithm	TP	FP	FN	P	R	F ₁	time
Random	500	PKBIC	88.900(3.144)	47.780(5.144)	20.100(3.144)	0.651(0.025)	0.816(0.029)	0.724(0.022)	4.321
		Or-PPGM	65.520(4.137)	3.420(1.679)	43.480(4.137)	0.951(0.023)	0.601(0.038)	0.736(0.029)	3.224
		Or-LPGM	64.380(3.833)	2.580(1.527)	44.620(3.833)	0.962(0.022)	0.591(0.035)	0.731(0.029)	0.239
		PDN	84.820(3.652)	494.120(20.495)	24.180(3.652)	0.147(0.008)	0.778(0.034)	0.247(0.013)	4.825
		ODS	44.040(4.458)	84.660(10.809)	64.960(4.458)	0.344(0.038)	0.404(0.041)	0.371(0.036)	158.765
		PC	35.140(3.175)	25.520(2.816)	73.860(3.175)	0.579(0.039)	0.322(0.029)	0.414(0.032)	0.100
		MMHC	51.500(5.632)	96.420(9.476)	57.500(5.632)	0.349(0.040)	0.472(0.052)	0.401(0.043)	0.576
	1000	PKBIC	99.540(1.460)	32.820(5.336)	9.460(1.460)	0.753(0.031)	0.913(0.013)	0.825(0.020)	6.734
		Or-PPGM	82.040(3.084)	2.120(1.043)	26.960(3.084)	0.975(0.012)	0.753(0.028)	0.849(0.019)	4.152
		Or-LPGM	85.440(3.308)	0.120(0.328)	23.560(3.308)	0.999(0.004)	0.784(0.030)	0.878(0.019)	0.416
		PDN	93.960(2.725)	361.620(18.856)	15.040(2.725)	0.207(0.011)	0.862(0.025)	0.333(0.015)	6.445
		ODS	58.380(5.810)	74.780(8.115)	50.620(5.810)	0.439(0.045)	0.536(0.053)	0.482(0.048)	243.041
		PC	47.620(2.996)	31.480(3.032)	61.380(2.996)	0.602(0.034)	0.437(0.027)	0.506(0.029)	0.117
		MMHC	66.840(4.892)	79.260(7.537)	42.160(4.892)	0.458(0.037)	0.613(0.045)	0.524(0.039)	0.943
	2000	PKBIC	104.140(0.783)	22.820(4.801)	4.860(0.783)	0.821(0.031)	0.955(0.007)	0.883(0.019)	11.455
		Or-PPGM	91.900(2.323)	2.940(1.361)	17.100(2.323)	0.969(0.014)	0.843(0.021)	0.902(0.014)	6.229
		Or-LPGM	98.020(2.369)	0.040(0.198)	10.980(2.369)	1.000(0.002)	0.899(0.022)	0.947(0.012)	0.774
		PDN	97.560(1.864)	257.700(11.438)	11.440(1.864)	0.275(0.010)	0.895(0.017)	0.421(0.012)	9.936
		ODS	66.440(4.625)	70.460(7.276)	42.560(4.625)	0.486(0.039)	0.610(0.042)	0.541(0.040)	385.807
		PC	57.540(3.303)	35.100(2.150)	51.460(3.303)	0.621(0.025)	0.528(0.030)	0.571(0.027)	0.141
		MMHC	76.400(4.412)	64.420(7.680)	32.600(4.412)	0.544(0.040)	0.701(0.040)	0.612(0.039)	1.797

D.2 Figure

Figure D.1, and Figure D.2 plot Precision P, and Recall R for each of methods considered in Section 5 of the main paper and for the three types of networks. Two different graph dimensions, i.e., $p = 10, 100$, and three graph structures (see Figure 1 and Figure 2 in the main paper) are considered.

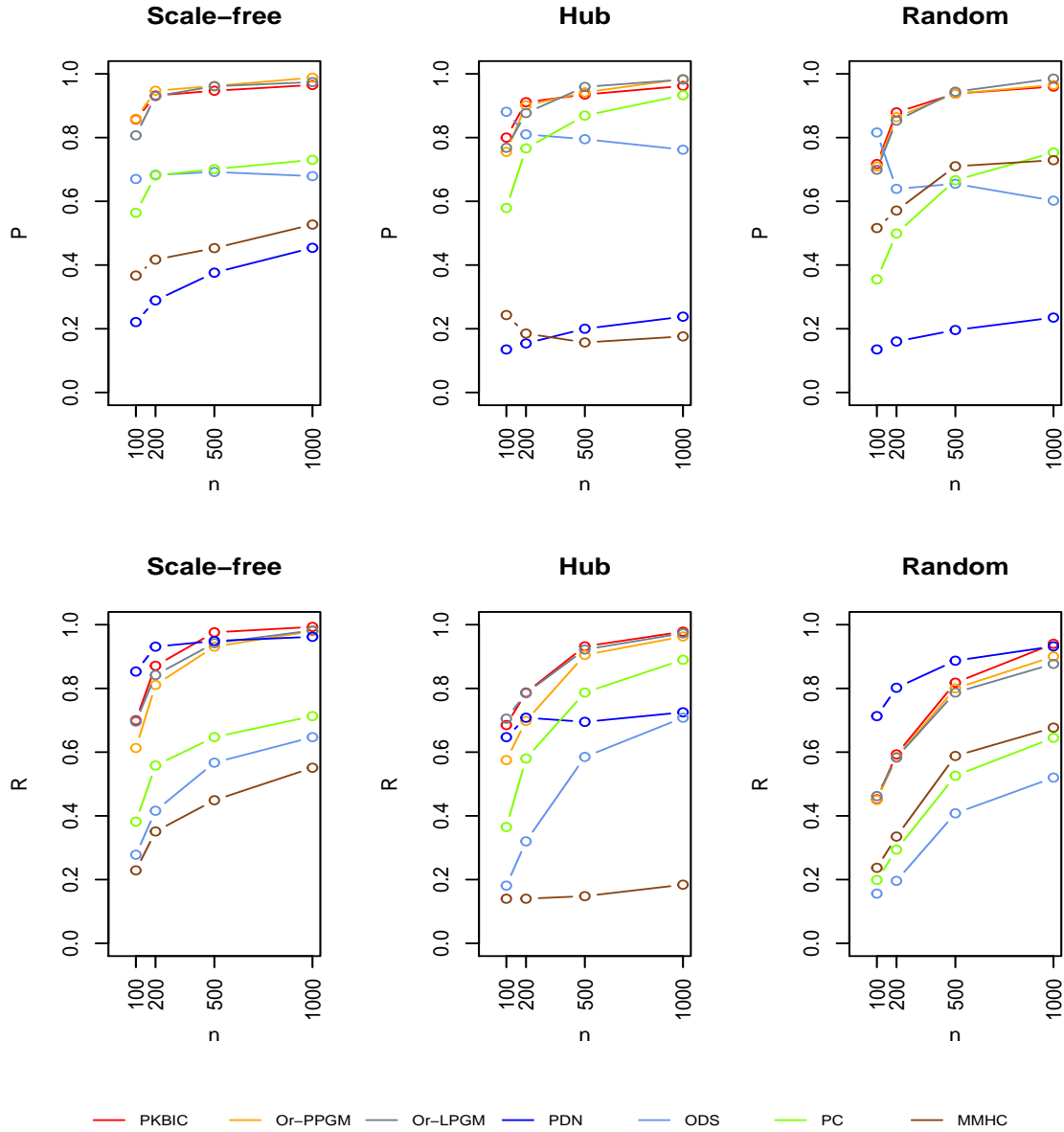


FIGURE D.1 Precision P , and Recall R of the considered algorithms: PKBIC; Or-PPGM; Or-LPGM; PDN; ODS; MMHC; and PC for the three types of graphs in Figure 1 of the main paper with $p = 10$ and sample sizes $n = 100, 200, 500, 1000$.

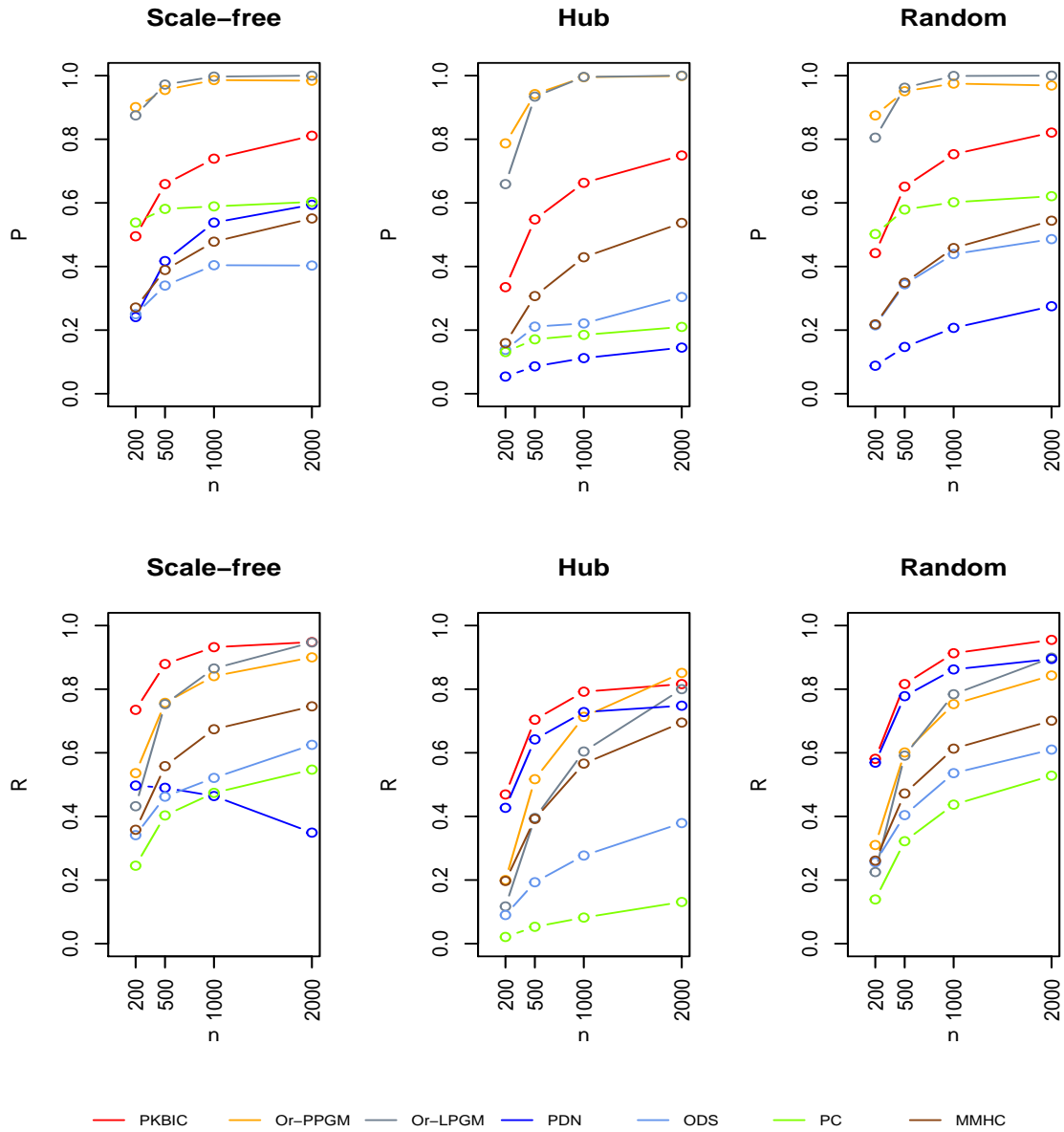


FIGURE D.2 Precision P, and Recall R of the considered algorithms: PKBIC; Or-PPGM; Or-LPGM; PDN; ODS; MMHC; and PC for the three types of graphs in Figure 2 of the main paper with $p = 100$ and sample sizes $n = 200, 500, 1000, 2000$.

References

- Akaike, H. (1974). A new look at the statistical model identification. *IEEE transactions on automatic control*, 19(6), 716–723.
- Allen, G., & Liu, Z. (2013). A local Poisson graphical model for inferring networks from sequencing data. *NanoBioscience, IEEE Transactions on*, 12(3), 189–198.
- Bühlmann, P., Peters, J., & Ernest, J. (2014). CAM: causal additive models, high-dimensional order search and penalized regression. *The Annals of Statistics*, 42(6), 2526–2556.
- Chickering, D. M., & Meek, C. (2002). Finding optimal Bayesian networks. In *Proceedings of the eighteenth conference on uncertainty in artificial intelligence* (pp. 94–102).
- Cooper, G. F., & Herskovits, E. (1992). A bayesian method for the induction of probabilistic networks from data. *Machine learning*, 9(4), 309–347.
- Djordjilović, V., Chiogna, M., & Vomlel, J. (2017). An empirical comparison of popular structure learning algorithms with a view to gene network inference. *International Journal of Approximate Reasoning*, 88, 602–613.
- Dor, D., & Tarsi, M. (1992). A simple algorithm to construct a consistent extension of a partially oriented graph. Technical Report R-185, Cognitive Systems Laboratory, UCLA.
- Fraley, C., & Raftery, A. E. (2002). Model-based clustering, discriminant analysis, and density estimation. *Journal of the American Statistical Association*, 97(458), 611–631.
- Gale, N. W., Kaplan, S., Lowenstein, E. J., Schlessinger, J., & Bar-Sagi, D. (1993). Grb2 mediates the egf-dependent activation of guanine nucleotide exchange on ras. *Nature*, 363(6424), 88–92.
- Gallopín, M., Rau, A., & Jaffrézic, F. (2013). A hierarchical poisson log-normal model for network inference from rna sequencing data. *PloS one*, 8(10), e77503.
- Hadji, F., Molina, A., Natarajan, S., & Kersting, K. (2015). Poisson dependency networks: Gradient boosted models for multivariate count data. *Machine Learning*, 100(2-3), 477–507.
- Haughton, D. M., et al. (1988). On the choice of a model to fit data from an exponential family. *The Annals of Statistics*, 16(1), 342–355.
- Hoeffding, W. (1963). Probability inequalities for sums of bounded random variables. *Journal of the American statistical association*, 58(301), 13–30.
- Hue Nguyen, T. K., & Chiogna, M. (2018, October). Structure learning of undirected graphical models for count data. *ArXiv e-prints*.
- Johnson, C. R., & Robinson, H. A. (1981). Eigenvalue inequalities for principal submatrices. *Linear Algebra and its Applications*, 37, 11–22.
- Kalisch, M., & Bühlmann, P. (2007). Estimating high-dimensional directed acyclic graphs with the PC-algorithm. *Journal of Machine Learning Research*, 8(Mar), 613–636.
- Kanehisa, M., & Goto, S. (2000). KEGG: Kyoto Encyclopedia of Genes and Genomes. *Nucleic Acids Research*, 28(1), 27–30. Retrieved 2012-06-08, from <http://www.ncbi.nlm.nih.gov/pubmed/10592173>
- Lauritzen, S. L. (1996). *Graphical Models* (Vol. 17). Clarendon Press, Oxford.
- Li, Y.-H., Scarlett, J., Ravikumar, P., & Cevher, V. (2015). Sparsistency of ℓ_1 -regularized m-estimators. In *Artificial intelligence and statistics* (pp. 644–652).
- Liu, H., Roeder, K., & Wasserman, L. (2010). Stability approach to regularization selection (stars) for high dimensional graphical models. In *Advances in neural information processing systems* (pp. 1432–1440).
- Nguyen, T. K. H., & Chiogna, M. (2021). Structure learning of undirected graphical models for count data. *Journal of Machine Learning Research*, 22(50), 1-53. Retrieved from <http://jmlr.org/papers/v22/18-401.html>
- Park, G., & Raskutti, G. (2015). Learning large-scale Poisson DAG models based on overdispersion scoring. In *Advances in neural information processing systems* (pp. 631–639).
- Peters, J., & Bühlmann, P. (2013). Identifiability of Gaussian structural equation models with equal error variances. *Biometrika*, 101(1), 219–228.
- Ravikumar, P., Wainwright, M. J., & Lafferty, J. D. (2010, 06). High-dimensional Ising model selection using ℓ_1 -regularized logistic regression. *The Annals of Statistics*, 38(3), 1287–1319.
- Sales, G., Calura, E., Cavalieri, D., & Romualdi, C. (2012). graphite-a bioconductor package to convert pathway topology to gene network. *BMC bioinformatics*, 13(1), 1–12.
- Schmidt, M., Niculescu-Mizil, A., & Murphy, K. (2007). Learning graphical model structure using ℓ_1 -regularization paths. In *Aaai* (Vol. 7, pp. 1278–1283).
- Schwarz, G. (1978). Estimating the dimension of a model. *The Annals of Statistics*, 6(2), 461–464.

-
- Teyssier, M., & Koller, D. (2005). Ordering-based search: A simple and effective algorithm for learning bayesian networks. In Proceedings of the twenty-first conference on uncertainty in artificial intelligence (p. 584–590). Arlington, Virginia, USA: AUAI Press.
- Tsamardinos, I., Brown, L. E., & Aliferis, C. F. (2006). The max-min hill-climbing Bayesian network structure learning algorithm. *Machine learning*, 65(1), 31–78.
- Wagenmakers, E. J., & Farrell, S. (2004). AIC model selection using Akaike weights. *Psychonomic Bulletin & Review*, 11(1), 192–196.
- Xue, J. Y., Zhao, Y., Aronowitz, J., Mai, T. T., Vides, A., Qeriqi, B., . . . Lito, P. (2020). Rapid non-uniform adaptation to conformation-specific kras (g12c) inhibition. *Nature*, 577(7790), 421–425.
- Yang, E., Allen, G., Liu, Z., & Ravikumar, P. K. (2012). Graphical models via generalized linear models. In *Advances in neural information processing systems* (pp. 1358–1366).
- Yang, E., Ravikumar, P., Allen, G. I., & Liu, Z. (2015). Graphical models via univariate exponential family distributions. *Journal of Machine Learning Research*, 16(1), 3813–3847.